OPTIMIZATION OF BRAKE PAD GEOMETRY TO PROMOTE GREATER CONVECTIVE COOLING TO INCREASE HEAT DISSIPATION RATE

By

Daryl Paul Premkumar

B.S., Southern Illinois University, 2016

A Thesis

Submitted in Partial Fulfillment of the Requirements for the degree of

Master of Science in Mechanical Engineering

Department of Mechanical Engineering and Energy Processes

Graduate School

Southern Illinois University Carbondale

May 2018

THESIS APPROVAL

OPTIMIZATION OF BRAKE PAD GEOMETRY TO PROMOTE GREATER CONVECTIVE COOLING TO INCREASE HEAT DISSIPATION RATE

By

Daryl Premkumar

A Thesis Submitted in Partial

Fulfillment of the Requirements

for the Degree of

Master of Science

in the field of Mechanical Engineering and Energy Processes

Approved by:

Dr. Peter Filip, Chair

Dr. Tsuchin Chu

Dr. Rasit Koc

Graduate School

Southern Illinois University Carbondale

March 30, 2018

AN ABSTRACT OF THE THESIS OF

Daryl Premkumar, for the Master of Science degree in Mechanical Engineering and Energy Processes, presented on March 30, 2018 at Southern Illinois University Carbondale.

TITLE: OPTIMIZATION OF BRAKE PAD GEOMETRY TO PROMOTE GREATER CONVECTIVE COOLING TO INCREASE HEAT DISSIPATION RATE

MAJOR PROFESSOR: Dr. Peter Filip

Despite many research pieces on brake systems, there is still research to be done on brake pad geometry and the dissipation of heat during brake engagements using the finite element analysis method. Brake application is a process in which the kinetic energy of the vehicle is mostly converted into thermal energy and then dissipated in the form of heat. Based on dynamometer test results it was seen that brake pad temperatures could reach up to 600° C [23]. Preliminary research using computer modeling software has shown that heat dissipation in brake pads with wavy geometries and air channels from the top to bottom is much better compared to pads that do not have those specific features. Brake pads that dissipate heat faster are prone to brake fade and other braking issues that may arise due to overheating [15]. For this research, two readily available brake pads and two designs of brake pads with new geometry were modeled using CAE software. Finite element analysis was then performed to test how well each brake pad dissipated heat after reaching brake fade temperatures. The readily available brake pads were from Power Stop and Wagner [26]. ANSYS Space Claim [25] was used to design and model the brake pads, ANSYS 18.2 [24] was used to perform the finite element analysis on the pads. After performing the analysis, results indicate that a brake pad with a design that had zones for turbulent air at ambient conditions and convection slots from the top to the bottom decreased in

temperature by about 90° C more in the same time compared to the conventional design. By studying the changing values of the convection heat transfer coefficient with velocity, the placing of the turbulence zones can be more precise in order attain greater airflow to remove heat from the brake pad quicker.

ACKNOWLEDGMENTS

First and foremost, I would like to thank my committee members. My committee chair Dr. Peter Filip has been instrumental in this study. His suggestions helped improve the standard of this thesis. Dr. Tsuchin “Philip” Chu always made himself available and provided suggestions on how to improve the model and simulation methodology. Dr. Rasit Koc, for his overall support and advise along the way. I would also like to thank Dr. Emmanuel Nsofor for his guidance in the heat transfer portion on this study and Mike Behrmann, the chair of the automotive center for helping with testing.

I would also like to thank Mr. Tom Venis from Tom’s Garage for providing brake samples that helped in initial modeling stages. During the initial stages of this study, Mr. Venis also shared his experience on different brake pad manufacturers and what to look out for when carrying out this study.

Finally, I would like to thank my family and friends for their unconditional love and support. This study would not have been possible without them.

DEDICATION

This thesis is dedicated to my family Dr. David Jayakumar, Mrs. Perlin David, Dr. Diana Priya, Dr. Jaganathan and Mr. Donovan Moses, for their constant love and support. Words cannot express how grateful I am to have them in my life. They've played the most important role in me getting where I am today.

This is also dedicated to Mr. Tom Venis and Mrs. Sheryl Venis. I cannot begin to describe how fortunate I am to have met such great people. Spending the weekends and holidays and eating great food with them gave me some resemblance of family in the United States.

I would also like to dedicate this to Stephanie Venis for always seeing the best in me, even during the times I could not. She made the long nights and tough deadlines much more bearable. She ensured I always produced quality work and was always there for love and support.

I want to also dedicate this to my boss, Scott Parroné, for teaching me some of the most important lessons in my life.

Finally, this is also dedicated my friends Suddarsun Shivakumar, Eric Lim and Daniel Cleary for walking the path of graduate school with me. Thank you for all your support.

TABLE OF CONTENTS

Chapter Page

LIST OF TABLES

LIST OF FIGURES

CHAPTER 1 - INTRODUCTION

1.1 BRAKE SYSTEM OVERVIEW

Brake systems are one of the most critical safety components in a vehicle. It is used to decrease the velocity of a vehicle with the help of aerodynamic drag. There are two main braking systems in modern vehicles. The first is the disk braking system and the other is the drum braking system. For this study, the disk braking system is going to be analyzed. While it is understood that aerodynamic drag and engine braking can be used to decrease the velocity of a vehicle, this research is mainly focusing on how the disk brake system with optimized brake pad designs decrease the velocity of the vehicle.

Whenever a driver needs to decrease the velocity of the vehicle instantaneously, the brake pedal is pressed causing brake pads to clamp onto the rotor to slow it down. The act of these two surfaces rubbing against each other is known as friction. This friction process operates by converting kinetic energy of the vehicle into thermal energy. Vehicle mass, velocity, and deceleration are factors in the heat generated in a friction braking system. During this process, a high amount of heat is generated and the temperature of both the pads and the rotors can be calculated to reach about 650° C [10]. The main aim of this study is to develop a brake pad with an optimized design that will be able to dissipate heat faster.

An optimized brake pad design that promotes greater convective cooling will cause the heat to be dissipated faster. This proposed study will use advanced computer modeling analysis software to optimize brake pad designs. For this study, brake pads from Wagner [22] and Power Stop [23] will be used for modeling and analysis. These two pads are meant for the Ford F-150

Regular Cab 6.5’ Box XL RWD 2-Door Pickup. Based on the results obtained for the analysis of these pads a new design will then be produced. The aim for the new design is to cool significantly faster after a brake engagement compared to the Wagner [26] and PowerStop brake pads.

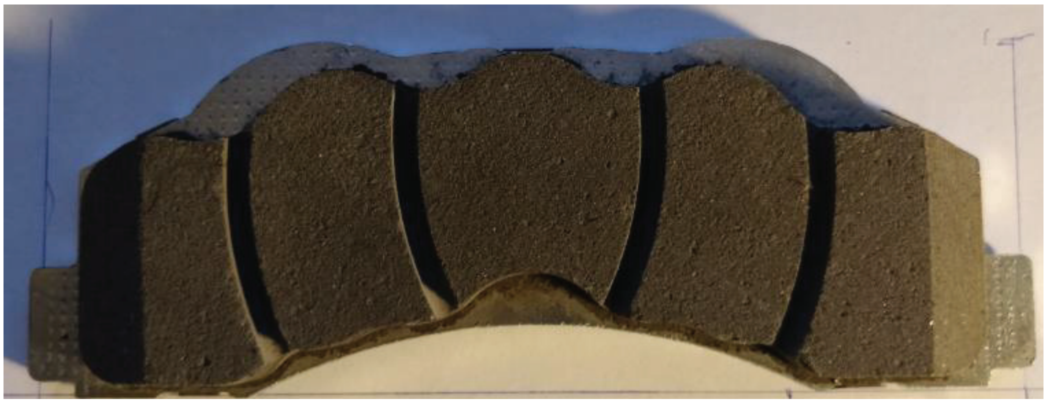

Figure 1.1: Wagner brake pad

Figure 1.2: Power Stop Brake Pad

Figure 1.3: Ford F150 for testing

The software that is going to be used for modeling, analysis and simulation is especially important, because the model must accurately depict real-world applications as braking systems in vehicles are critical safety components. ANSYS Space Claim [25] which is known for its ease of use when modeling mechanical devices, is the primary option as it has all the features required to model the brake pad as accurately as possible. For the simulation software, ANSYS 18.2 [24] was chosen because of the multiple types of analysis that can be run on the pad (eg. steady state analysis, transient state analysis, coupling of pad and rotor, von-misses stress, strain, etc.). ANSYS 18.2 [24] is also known to be widely used in industry and yields accurate results [10]. ANSYS 18.2 [24] also has an inbuilt optimization tool that can aid in the final design. The optimization tool performs numerical analysis to determine areas where mass can be shaved and areas where mass needs to be added.

By improving the heat dissipation in the brake pad, the temperature on the surface after brake engagement decreases quickly, therefore preventing brake fade [9]. Brake fade is the temporary reduction or complete loss of braking power of a vehicle's braking system. Brake fade occurs when the brake pad and the brake rotor no longer generate sufficient mutual friction to stop the vehicle at its preferred rate of deceleration. The result being inconsistent or unexpected braking system behavior, often resulting in increased stopping distances [13]. It is also expected that by improving heat dissipation, the brake pad life will be increased and the environmental effect will be lessened as demonstrated by Grigoratos, et. al [6]. It is expected that a design with slots through the center and a wavy geometry on the top and bottom portion of the brake pad will create a zone of turbulent air that will cool the brake pad faster. This research will further advance the knowledge in turbulent air zones as well as improve the design of slots on the face of the brake pad to achieve greater heat dissipation.

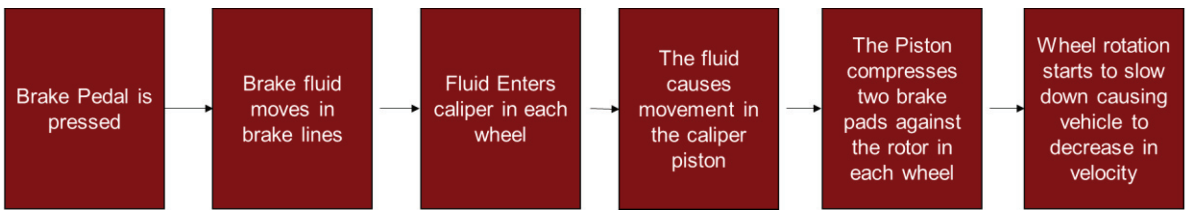

Figure 1.4: The Braking Process

CHAPTER 2 - LITERATURE REVIEW

2.1 LITERATURE REVIEW

Braking systems in vehicles are energy conversion tools. They convert the kinetic energy of the vehicle into heat energy through friction [7]. This is in addition to the aerodynamic drag that the vehicle experiences. However, if the brake pad is subject to high temperatures for a long period of time, the stopping power decreases, and the life of the brake pad becomes significantly reduced [1,2]. Timur et al [3] studied the temperature-stress distribution during braking by different brake pad materials. It was found that a brake pad with specified wear had a higher maximum and minimum temperature during the braking process compared to new non-wore pad of the same material going through the exact same braking process. Belhocine et al [4] presented a numerical simulation of the thermal behavior of a full and ventilated disk. This study also demonstrated the pressure distribution in brake pads at different stages of brake application. Belhocine's study provides the foundation for this research as it has set the basic parameters to perform the analysis; while Belhocine's study mainly analyses the rotor, this research analyzes the brake pad.

Talati et al. [5] demonstrated heat conduction in braking systems. In his paper, the governing equations in the brake disk and pad were extracted in the form of transient heat equations with heat generation that was dependent on time and space. Talati also stated that long, repetitive braking leads to excessive temperature increase in various brake components of the vehicle that leads to a reduction in performance of the vehicle. Gao and Lin [8] presented an analytical model to determine the contact temperature distribution on the working surface of a brake. To consider the effects of the moving heat source (the pad) with relative sliding speed variation, a transient finite element technique is used to characterize the temperature fields of the solid rotor with appropriate thermal boundary conditions. Numerical results show that the operating characteristics of the brake exert an essential influence on the surface temperature distribution and the maximum contact temperature.

Voldrich et al. [9] concluded that non-uniform contact pressure distribution and formation of hot spots is a negative effect that are apparent in disk brakes during brake engagement. Voldrich also demonstrated that if the sliding velocity was high enough it can cause the brake assembly to become unstable and could result in disk material damage, frictional vibration and uneven wear in the brake pad.

Reddy et al. [10] used ANSYS [24] to mesh and analyze the car brake disk. This research piece demonstrates the steps when performing finite element analysis using ANSYS [24]. In Reddy's research, he outlines the necessary steps for analysis using ANSYS [24]. He describes the first step as preliminary decisions where the analysis type is determined, the model is fixed and the element type is specified, then he moves on to preprocessing where the material is specified and the geometry of the model is created or imported. At this stage, the meshing of the model is performed, Reddy particularly highlights the use of a fine mesh to have accurate results. The third step is to apply the thermal loads, heat flux and convection cooling and then solve the model. Then, as part of post processing, the results are reviewed and the validity of the solution is assessed.

In the article, *Structural and Thermal Analysis of Rotor Disc of the Disc Brake* by Manjunath et al. [11] he demonstrated the thermomechanical behavior of the dry contact of the brake disc during brake engagement. The coupled thermal-structural analysis was then used to determine the deformation and the Von Mises stress. Manjunath compares two similar brake disk designs with different materials. He also specifies that for most vehicles the axle weight distribution is about 70% for the front of the vehicle and 30% for the back of the vehicle. While Manjunath approaches the calculation in a different way for this study, his calculations can be used as a comparison for this research.

As can be seen from the above literature review, a lot of research has been done on brake rotor performance, as well as heat dissipation in brake rotors. While there has been some research of the brake pad, it is mostly based on the contact pressure and material transfer with the rotor. With the exception, of Cheng Liu et al. [12] who researched the effect of chamfered brake pad patterns on the vibration squeal response of disc brake system. There is not a lot of research that has been done with respect to pad geometry using FEA and even then, Cheng's research is to analyze squeal response instead of heat dissipation. This present study aims to create a new brake pad design with a complex geometry that is capable of dissipating heat faster than readily available brake pads. This will increase the overall brake pad life, decrease brake fade, and decrease the harmful effect on the environment.

2.2 BRAKE ISSUES THAT ARE ASSOCIATED WITH OVERHEATING

There is more to a braking system than just a pad and rotor. The other components include, the brake pedal, booster cylinder, ABS module, brake line, brake fluid, and caliper. If the operating temperatures for any one of these components are exceeded, it may result in a partial loss of brake function and in severe cases complete loss of brakes. It can be difficult to attribute thermal brake failure to motor vehicle accidents as normal braking operation may return to the vehicle when the temperatures return to below their critical level [14]. Brake Fade is a common problem that is caused by high temperatures. Other problems include brake judder (thermally excited vibration) and rotor deterioration [15]. Excessive heat from surrounding components can also lead to brake fluid vaporization, damaged seals, wheel bearing damage and radiated heat can cause damage to the tire at temperatures as low as 93° C, [15], [16].

2.3 HEAT DISSIPATION FROM BRAKE PADS IN BRAKE DISK SYSTEMS

Factors such as vehicle mass, initial velocity, deceleration rate, aerodynamic drag, rolling resistance and brake ratio contribute to the rise in brake pad temperature during brake application. For brake applications with short periods and low decelerations, the friction material and rotor may absorb all the thermal energy generated and result in low heat dissipation as the temperature rise is minimal [15]. However, in repeated high-speed brake applications, it is critical to dissipate the heat at a quick rate to ensure optimal brake performance.

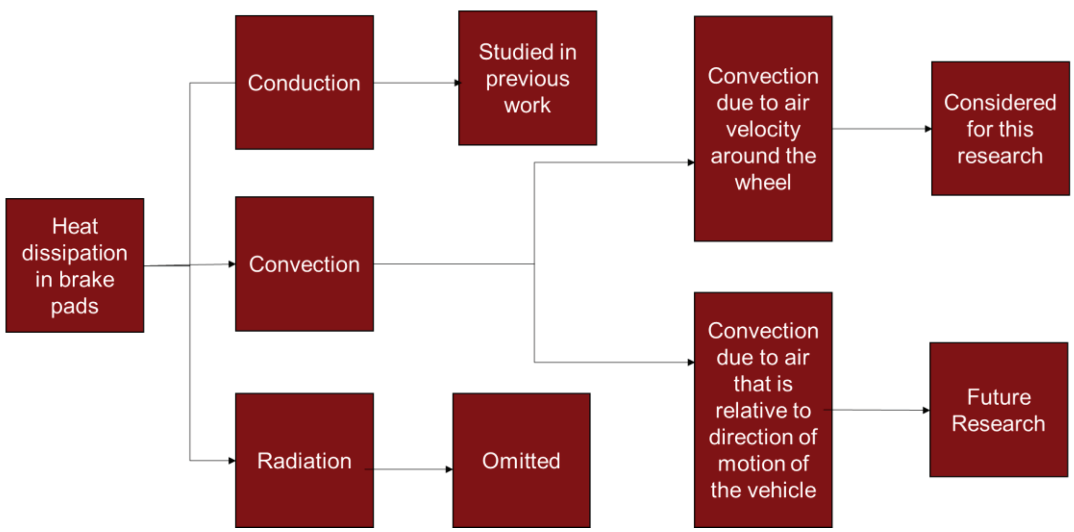

Figure 2.3.1: Heat Transfer Flow chart

The three modes of heat transfer in brake applications are conduction, radiation and convection. Conduction occurs through the brake assembly and hub, radiation will cause nearby components to increase in temperature and convection dissipates the heat to the air. While radiation heat transfer has its greatest effect at high temperatures, it is controlled to prevent tire overheating [15], [16]. Heat dissipated through radiation can also be calculated to be around 5% of the total heat dissipated. The primary objective of this study is the heat dissipation through convection to the atmosphere.

CHAPTER 3 - OBJECTIVES

3.1 STATEMENT OF OBJECTIVES

1) Model the friction process of braking based on the coefficient of friction.
2) Model how heat is dissipated in different pad geometries.
3) Optimize the shape of the brake pad to promote greater convective cooling.

CHAPTER 4 – EXPERIMENTAL METHODS

4.1 LIST OF SYMBOLS

E	Energy (J)
F_f	Friction force (N)
ΔX	Sliding distance (m)
μ_f	Coefficient of friction (dimensionless)
F_N	Normal Load (N)
P	Pressure (pa)
A	Area (m^2)
Q	Heat (J)
r_r	Rotor Radius (m)
r_w	Wheel Radius (m)
d_w	Sliding distance of wheel (m)
d_r	Sliding distance of rotor (m)
M	Mass (kg)
V_0	Initial Velocity ($m\ s^{-1}$)
V_f	Final Velocity ($m\ s^{-1}$)
t	time (s)
a	acceleration ($m\ s^{-2}$)
c	Specific Heat ($J\ kg^{-1}\ K^{-1}$)
h	Heat transfer coefficient ($W\ m^{-2}\ K^{-1}$)
T	Temperature (° C)
k	Thermal Conductivity ($W\ m^{-1}\ K^{-1}$)
g	Gravitational acceleration ($m\ s^{-2}$)
FEA	Finite Element Analysis

4.2 APPROACH USING KINETIC ENERGY

The best possible method to determine the temperature rise due to energy conversion is by using the Kinetic energy equation approach. This approach allows for the deceleration due to rolling resistance and aerodynamic drag to be calculated and factored in to the energy equation.

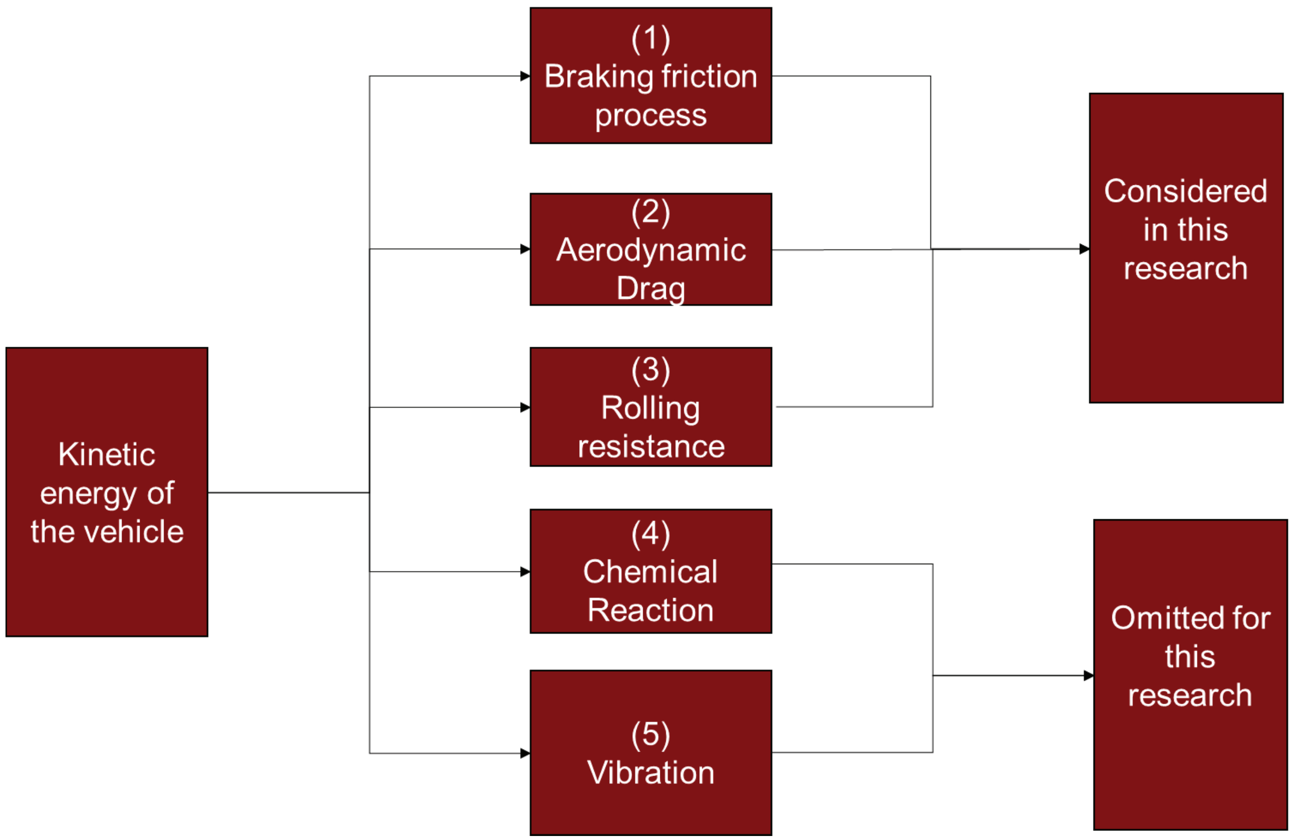

Figure 4.1: Flowchart of kinetic energy dissipation

For this approach, the velocity that will be used in the final energy equation is (ΔV). This will help when determining the variation of energy and temperature with respect to time. The data that shows the respective velocities, temperatures, and energy with respect to time is included in the appendix. Due to the nature of this transient problem, numerical techniques were used to find the changing values with respect to time. The following calculations are an example of one segment of those values. For demonstration purposes, the parameters when t = 0.25 (s) will be calculated.

The first coefficient that must be determined is the coefficient of rolling resistance C_{rr}. Because the coefficient of rolling resistance C_{rr} is a function of vehicle velocity it can be expected to change over the acceleration/deceleration of the vehicle. Using equation (1), C_{rr} can be found.

$$\mathrm{Crr} = 0.005 + \frac{1}{P} * (0.01 + 0.0095 * (\frac{V}{100})^2 \quad (1)$$

The tire pressure is assumed to be 2.5 bar and the velocity of the vehicle is 100 km/h.

$$\mathrm{Crr} = 0.005 + \frac{1}{2.5\ bar} * (0.01 + 0.0095 * (\frac{100km/h}{100})^2 = 0.01280608$$

Based on these set parameters, the coefficient of rolling resistance C_{rr} is found to be 0.01280608. Once the coefficient of rolling resistance C_{rr} is determined, the force due to rolling resistance, F_{rr} can be calculated using the following equation:

$$Frr = Crr * m * g \ (2)$$

Where m =2.045.45 kg and g = 9.81 m/s

$$Frr = 0.01280608 * 2045.45\ kg * 9.81 \frac{m}{s} = 256.965\ N$$

Once the Force due to rolling resistance is found, the force due to drag must be calculated. Based on data from the Eco Modder website the coefficient of drag for the Ford F-150 can be assumed to be 0.4. Using equation (3) the drag force, F_d can be calculated

$$Fd = \frac{1}{2} * p * v^2 * Cd * A \ (3)$$

Where

p = mass density of the fluid which is air, 1.225 kg/m^3

v = Speed of object with respect to fluid, 26.71 m/s

Cd = Drag Coefficient, 0.4

A = Projected front area of vehicle, 2.94 m^2

$$F_D = \frac{1}{2} * 1.225 \frac{\text{kg}^3}{\text{m}} * 26.71 \frac{\text{m}^2}{\text{s}} * 0.4 * 2.94m^2 = 514.2471\ N$$

By summing the drag force, F_d and the force due to rolling resistance, F_{rr} the total resisting force without brake application is determined. Based on the value of the force, the acceleration can be calculated using the following equation.

$$a = \frac{F}{M} \quad (4)$$

$$a = \frac{771.2\ (N)}{2045.45\ (kg)} = -\ 0.3770\ m/s^2$$

A minus sign is be added to the acceleration, as it acts in the opposite direction to the motion of the vehicle.

For this specific case, AK-master deceleration parameters of 0.4g are assumed. Therefore, the total deceleration at t =0.25(s) is calculated to be

$$a = -(0.4 * 9.81)\frac{m}{s^2} + (-0.3770)\frac{m}{s^2} = -4.301\ m/s^2$$

Once the acceleration factor has been determined, the velocity at t= 0.25(s) can be calculated using equation (5).

$$Vf = (a * t) + Vi \quad (5)$$

$$Vf = \left(-4.301\frac{m^2}{s} * 0.25\ (s)\right) + 27.8\ m/s = 26.71 \text{ m/s}$$

Based on the velocity at 0.25(s), the total energy released from the deceleration can be calculated using equation (6).

$$E = \frac{1}{2} * M * \Delta V^2 \quad (6)$$

$$E = \frac{1}{2} * (2045.45) * (27.8 - 26.7195548)^2 = 1193.5\ (J)$$

1193 Joules is the amount of energy released from the vehicle going from 27.8 m/s to 26.71 m/s. From equation (4), a certain portion of the deceleration is due to drag force and rolling resistance. Seeing that this study is only considering the effects of the temperature due to braking action, only a percentage of the energy will be used to calculate the change in temperature of the brake pad. This percentage is calculated by:

$$\frac{(a_{fd} + a_{frr})}{total\ acceleration} * 100$$

At t =0.25(s), this percentage is found to be

$$\left(\frac{-0.397780699}{-4.321780699}\right) * 100 = 9\%$$

Therefore, it can be said that after 0.25 seconds of initial brake application the force due to drag and rolling resistance account for 9% of the deceleration. Therefore 91% of the energy converted into heat is due to braking. Based on equation (6), only 91% of the energy will be considered

0.91 * 1193.5J = 1089.08 J

This value then can be split depending on the brake ratio between the front and the back of the vehicle. A 70:30 front braking to rear braking is assumed for this case. The energy values for the front and back can be calculated to be

$$Front = 0.7 * 1089.08 = 762.96\ (J)$$

$$Back = 0.3 * 1089.08 = 326.98\ (J)$$

The energy values are then assumed to be split equally between the left and right sides of the of the front and rear of vehicle respectively.

$$Front\ left\ and\ right\ respectively = \frac{762.96}{2} = 381.48\ J$$

$$Rear\ left\ and\ right\ respectively = \frac{326.98}{2} = 163.49\ J$$

Brake rotor = 28 lbs. = 12 kg

Brake pad = 3.3 lbs. = 1.5 kg

This equation will yield the kinetic energy of the vehicle dependent on the mass and the velocity of the vehicle. Based on the value attained for kinetic energy, we can then calculate the change in temperature by using the caloric heat equation.

$$Q = m * c_p * (\Delta T)\ (23)$$

Where

$$(\Delta T) = \frac{Q}{m * c_p}$$

where Q is the energy in Joules, m is the mass of the object, Cp is the specific heat capacity and ΔT is the difference in temperature. Temperature change in the brake pad at 7 seconds (1 brake engagement) is calculated to be

$$(\Delta T) = \frac{276176}{1.4 * 900} = 219\ {}^{0}C$$

This temperature is then divided in half as there is an inner and outer pad.

$$(\Delta T)_{single\ pad} \frac{204.57}{2} = 109.5\ {}^{0}C$$

The final temperature that is entered in for the analysis also accounts for ambient air. For demonstration purposes, T_{amb} = 20ºC which puts the brake pad temperature at 122.29ºC after 1 engagement from 100 km/h to 5 km/h.

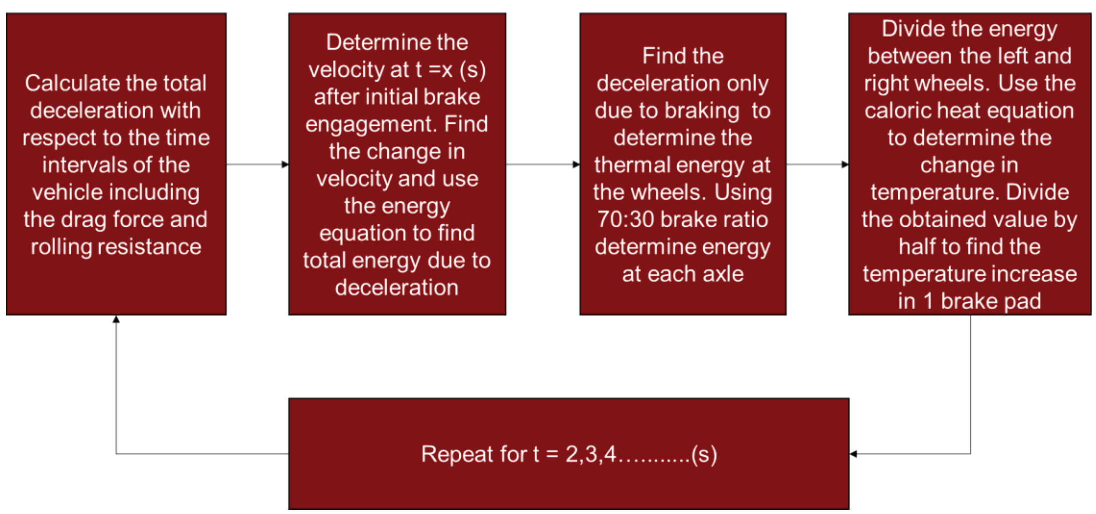

Figure 4.2: Heating flow chart activity

The method used to calculate cooling on the brake pad surface is based on the convective heat transfer formula. This method allows us to break down the flow of air over the entire pad into small channels, which is the exact requirement for this study.

To determine the cooling rate, first the film temperature will need to be determined, the film temperature is used to determine the properties of air at various braking phases. These properties are then used to determine the type of flow based on temperature.

The following equation is used to determine the film temperature:

$$T_{Film} = \frac{T_S + T_\infty}{2} \qquad (9)$$

where T_s is the temperature at the surface of the object and T_∞ is the ambient temperature?

For this calculation, the following assumptions were made

(1) The ambient temperature is 20° C

(2) The brake pad surface temperature is 175.96 ° C

(3) The velocity of the vehicle is 20 m/s

The film temperature is determined to be:

$$T_{Film} = \frac{175.96 + 30}{2} = 102.98\ ^0C$$

By using the film temperature, we can then use the air property tables to determine the Prandtl number, Pr, the density of the fluid, ρ, the dynamic viscosity, μ and air thermal conductivity, k.

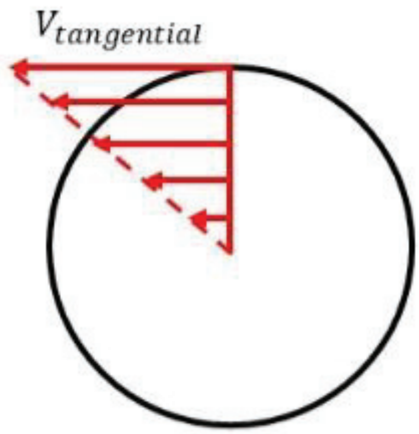

Figure 4.3: Tangential velocity of wheel

The velocity that is used in calculating the Reynolds number is determined using tangential velocity. The tangential velocity is calculated at specific radiuses and then the convective heat transfer coefficient is determined. The characteristic length is also a factor in determining the heat transfer coefficients at specific points on the brake pad. For FEA purposes, three types of convective heat transfer coefficients are considered. The overall convective heat transfer coefficient, the slot convective heat transfer coefficient and the rounded peak convective heat transfer coefficient. High velocity air flow that creates turbulence zones around the slots on the brake pad allow for faster moving cooling air which allow the for faster cooling of the brake pad.

By substituting the values obtained into the equation below, the type of flow can be determined.

$$Re_x = \frac{\rho * \upsilon * L}{\mu} \qquad (10)$$

$$Re_x = \frac{1.164 * 27.8 * 0.38}{0.00001872} = 6.57E + 05$$

Based on the Reynolds number obtained the flow can be classified into three types, laminar, transient or turbulent. The critical Reynolds number for this application is $5 \, x \, 10^5$, for flow that is lesser than this value the flow is classified as laminar, for flow in the range of the value it is classified as transitional and for flow above this value is it classified as turbulent.

Based the number of variables in the formulas required, multiple iterations will need to be done. The temperature as well as speed of air relative to the object changes throughout braking application, this change will yield different flow types which will vary the convective heat transfer coefficient. Based on the Reynolds number the equation to find the Nusselts number can be selected. If the flow is lesser than the critical Reynolds number it is classified as laminar and the flowing equation will be used:

$$Nu = 0.664 {Re_L}^{0.5} \, Pr^{1/3} \qquad (11)$$

If the flow is in the range of the critical Reynolds number the flow is classified as transient and the following equation will be used:

$$Nu = (0.037 {Re_L}^{0.8} - 871) \, Pr^{1/3} \qquad (12)$$

If the flow is greater than the critical Reynolds number the flow is classified as turbulent and the following equation will be used:

$$Nu = 0.037 {Re_L}^{0.8} \, Pr^{1/3} \qquad (13)$$

$$Nu = 0.037 * (6.57E+05)^{0.8} \, (0.7282)^{1/3}$$

Based on the Nusselt number obtained, the convective heat transfer coefficient, h can be determined based on the following equation:

$$h = \frac{k}{L} * Nu \quad (14)$$

$$h = \frac{0.02588}{0.38} * 1500 = 102.21 \text{ W/m2 } {}^{0}\text{C}$$

where h, is the convective heat transfer coefficient, k is the thermal conductivity, L is the characteristic length and Nu is the Nusselt number.

Based on this the rate at which heat needs to be dissipated with respect to convective heat transfer can be calculated. The general convective heat transfer equation is given as:

$$Q = h\,A\,(Tsurf - Tfluid) \quad (15)$$

Using numerical techniques, each value is calculated for every second the brake is engaged or released. The data charts are included in the appendix. The changing convective heat transfer rate is supplied to ANSYS [24] workbench along with the brake heating temperatures.

4.3 COMPUTING METHODOLOGY

1) The models of the brake pad are laid on a white background and the major dimensions (rectangle bounding box) around the pad. Images of the brake pads are taken and imported to the computer for processing.

Figure 4.3.1 : Wagner brake pad image

2) Once the images are processed, they are then imported into ANSYS SpaceClaim [25] to be modeled based on the image.

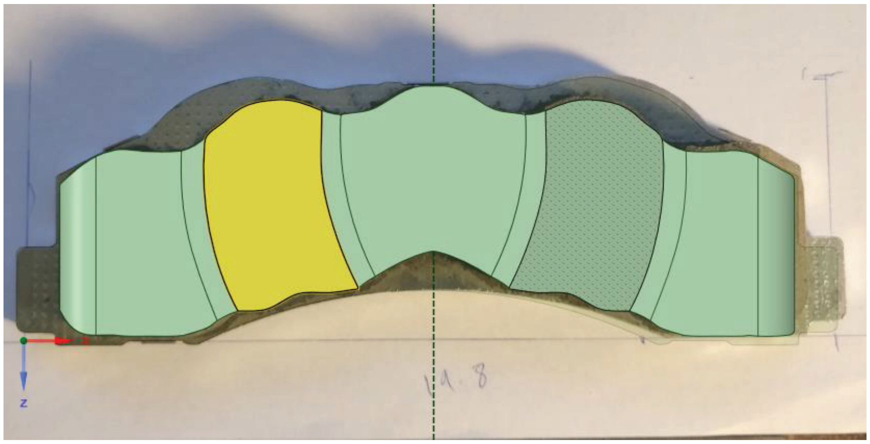

Figure 4.3.2 Modeled Wagner brake pad

3) In addition to Wagner [26] and PowerStop existing models and two other designs were modeled using ANSYS Space Claim [25].

4) Input the vehicle data into the created excel spreadsheet. Data such as acceleration, deceleration, mass, tire pressure, gravity, drag coefficient, exposed area, initial and final velocity, weight, ambient temperature, brake ratio and brake pad area is required. This tool will calculate the temperature rise in the brake pads. This table can be seen in the Appendix A.

5) To calculate the convective heat transfer coefficient for the brake pad, another spreadsheet was developed. Data such as linear velocity, wheel radius, and characteristic lengths for specific parts of the brake pads.

Table 4.3.1: Convective heat transfer coefficient calculated values

				Over all			Slots			Rounded Peaks		
Density	Dynamic Viscosity	Conductivity	Prandlt	ReyNolds	Nu	h	ReyNolds	Nu	h	ReyNolds	Nu	h
1.164	0.00001872	0.02588	0.7282	6.57E+05	484.06	32.967	2.80E+04	99.978	64.686	2.10E+04	86.583	74.69267
1.164	0.00001872	0.02588	0.7282	5.56E+05	445.48	30.34	2.37E+04	92.01	59.531	1.78E+04	79.683	68.74001
1.164	0.00001872	0.02588	0.7282	4.59E+05	404.79	27.568	1.96E+04	83.605	54.093	1.47E+04	72.404	62.46074
1.164	0.00001872	0.02588	0.7282	3.65E+05	360.73	24.568	1.56E+04	74.505	48.205	1.17E+04	64.524	55.66238
1.092	0.00001963	0.02735	0.7228	2.43E+05	293.76	21.143	1.04E+04	60.674	41.486	7.78E+03	52.545	47.90378
1.092	0.00001963	0.02735	0.7228	1.60E+05	238.66	17.178	6.85E+03	49.294	33.705	5.13E+03	42.69	38.91901
1.092	0.00001963	0.02735	0.7228	7.77E+04	166.04	11.95	3.31E+03	34.293	23.448	2.48E+03	29.699	27.07547
0.9994	0.00002096	0.02953	0.7154	1.29E+04	67.304	5.2303	5.48E+02	13.901	10.263	4.11E+02	12.039	11.85012
0.9994	0.00002096	0.02953	0.7154	12850.2579	67.304	5.2303	548.1827483	13.901	10.263	411.137	12.039	11.85012
0.9994	0.00002096	0.02953	0.7154	8.23E+04	170.28	13.233	3.51E+03	35.17	25.965	2.63E+03	30.458	29.9813
0.9994	0.00002096	0.02953	0.7154	1.51E+05	230.76	17.932	6.44E+03	47.661	35.186	4.83E+03	41.275	40.62883
0.9994	0.00002096	0.02953	0.7154	2.19E+05	277.62	21.574	9.33E+03	57.341	42.332	7.00E+03	49.659	48.88053
0.9994	0.00002096	0.02953	0.7154	2.84E+05	316.68	24.609	1.21E+04	65.407	48.287	9.10E+03	56.644	55.75671
0.9994	0.00002096	0.02953	0.7154	3.48E+05	350.31	27.223	1.49E+04	72.354	53.416	1.11E+04	62.661	61.67914
0.9994	0.00002096	0.02953	0.7154	4.09E+05	379.82	29.516	1.75E+04	78.448	57.914	1.31E+04	67.938	66.87341
0.9994	0.00002096	0.02953	0.7154	4.68E+05	405.98	31.549	1.99E+04	83.852	61.904	1.50E+04	72.618	71.4801
0.9994	0.00002096	0.02953	0.7154	5.23E+05	429.36	33.366	2.23E+04	88.681	65.469	1.67E+04	76.8	75.59654

6) Based on the information obtained, a value input spreadsheet was then developed to simplify calculations and ANSYS [24] value inputs.

Table 4.3.2: FEA Input information

Time(s)	Temperatures	Convective Over All	Convective Slots	Rounded Peaks
0	20	32.96691014	64.68574867	74.69266882
1	25.134	30.33959867	59.53059133	68.74000586
2	31.482	27.5681332	54.09258339	62.46073516
3	41.771	24.56756057	48.20503475	55.66237958
4	56.645	21.1431678	41.48589094	47.9037806
5	74.997	17.17758297	33.70485164	38.91901033
6	98.097	11.95023237	23.44804911	27.07547493
7	124.83	5.230259015	10.26250925	11.85012495
8	[redacted]	5.230259015	10.26250925	11.85012495
9	[redacted]	13.23276952	25.96456871	29.98130147
10	[redacted]	17.93224114	35.18559788	40.62882881
11	[redacted]	21.57427317	42.33178075	48.88053003
12	[redacted]	24.60919518	48.28672774	55.75671052
13	[redacted]	27.22316114	53.41569933	61.67913678
14	[redacted]	29.51574227	57.91406832	66.87340587
15	[redacted]	31.54898892	61.90358634	71.48010448

7) The model is then imported into ANSYS [24] and a transient thermal system is started.

8) The material properties are assigned in the engineering data tab.

Table 4.3.3: Engineering Data Inputs

	Density (kg/m^{-3})	Thermal Conductivity ($W\ m^{-1}\ C^{-1}$)	Specific Heat Capacity ($J\ kg^{-1}\ C^{-1}$)
Brake Pad	2680	0.5	900
Steel Backing Plate	8710	46	445

9) The mechanical module is then started. The material is then assigned its specified properties, e.g. brake pad, backing plate.

10) A mesh for the model is then generated. Because the copy of ANSYS [24] available was only meant for students. The combined number of nodes and elements could not exceed

32,000 for nodes and 16,000 for elements. The number of mesh nodes were constantly optimized to attain a value close to 32,000.

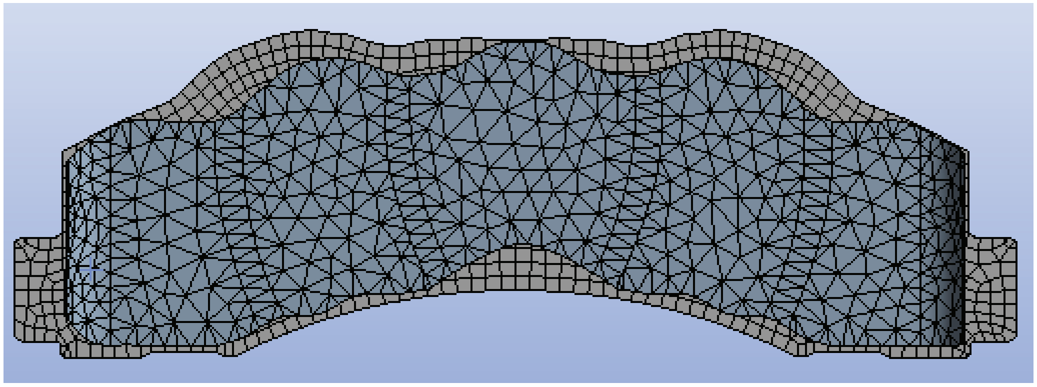

Figure 4.3.3: Mesh for Wagner Model

11) The temperature thermal load is then applied to the model. This load is based on the values calculated and simplified in step 6.

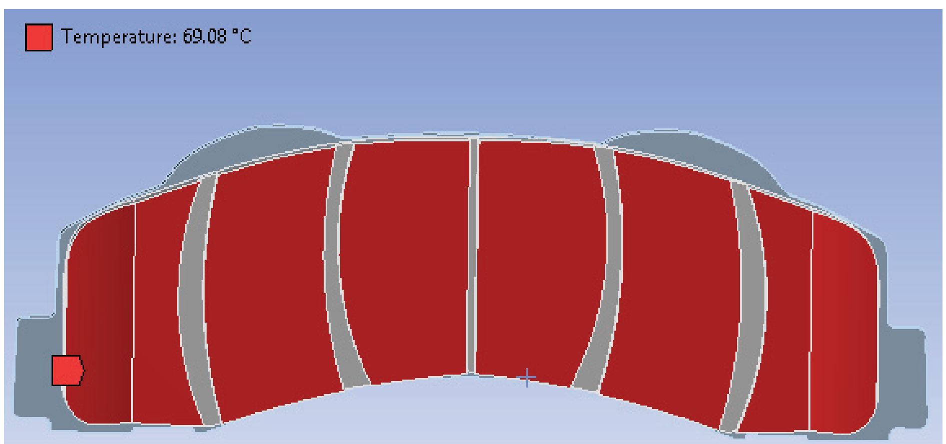

Figure 4.3.4: Temperature face of the brake pad

12) The convection information is then entered. The basis of this study was the impact of slots on the overall cooling, thus 2 convection categories were taken into consideration. The first was overall convection which was applied to the entire brake pad body and the second was slot convection, which was applied to the slots as well as the bodies

surrounding the slot. The information that was input into the software is based on the values calculated and simplified in step 6.

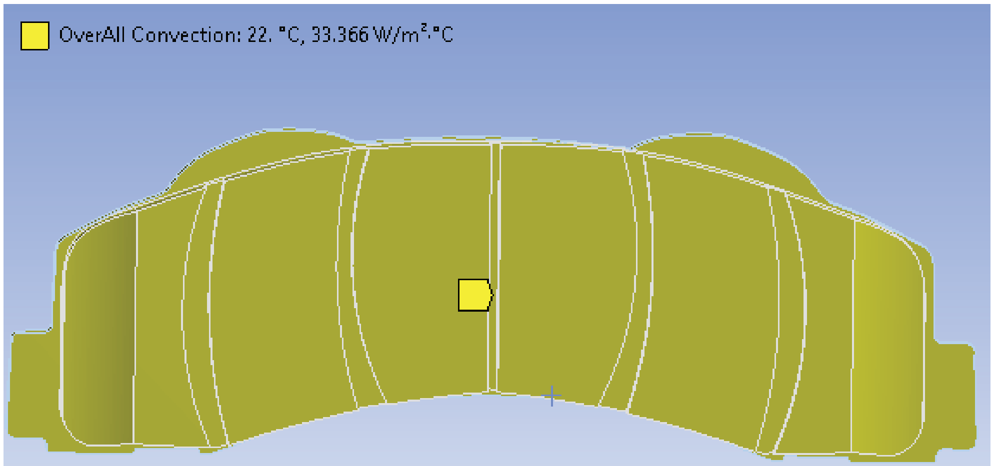

Figure 4.3.5: Overall convection

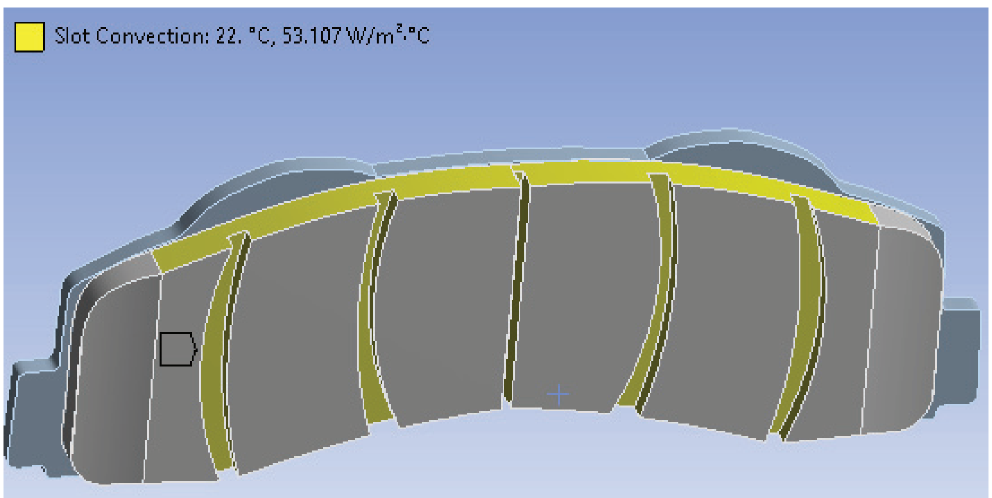

Figure 4.3.6: Slot convection

13) The time steps are for the analysis is then specified. The intervals for each analysis was 15 seconds. The start of each analysis was the engagement of the brake system, this means increasing the temperature of the brake pad for the 7 seconds of brake application

and then releasing the brakes and bringing the vehicle back up to speed and engaging the brakes again. This step is repeated until brake fade temperatures are reached.

Table 4.3.4: Temperature, time, convection coefficient Input data [25]

Tabular Data

	Steps	Time [s]	Temperature [°C]
1	1	0.	20.
2	1	1.	22.254
3	2	2.	28.85
4	3	3.	39.613
5	4	4.	54.454
6	5	5.	73.359
7	6	6.	96.385
8	7	7.	123.67
9	8	8.	123.67
10	9	9.	123.67

Convection Coefficient [W/m^2·°C]	Temperature [°C]
52.472	20.
48.29	20.
43.879	20.
39.103	20.
33.652	20.
27.341	20.
19.021	20.
8.3247	20.
21.062	20.
28.542	20.
34.339	20.
39.169	20.
43.33	20.

14) Heat flows to the brake pad for first 7 seconds of the engagement. The next 7 seconds are then deactivated as there is no heat being applied to the brake pad. The changing convection values are applied throughout the entire analysis.

15) At the end of the 15 seconds, the final brake temperature was input into the value inputs spreadsheet, temperatures for another full engagement were then added and the analysis was repeated it reached until fade temperatures.

16) The final brake pad temperature gradient was obtained

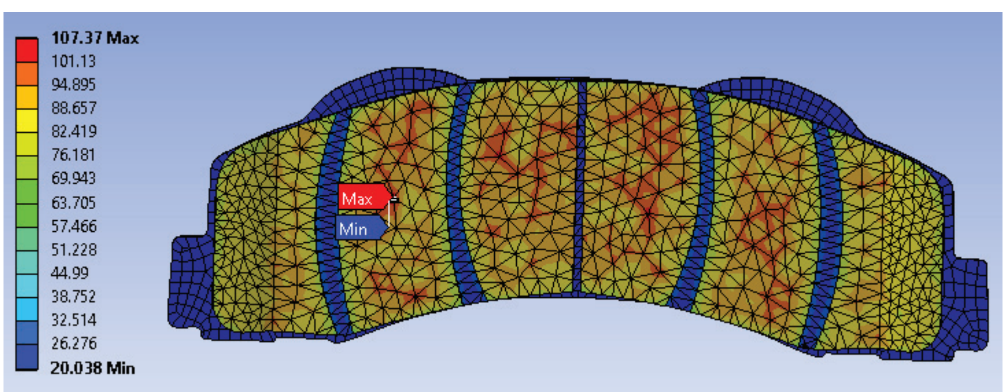

Figure 4.3.7: Temperature gradient of brake pad

17) This methodology was used on the newly designed brake pads and the new design was optimized accordingly.

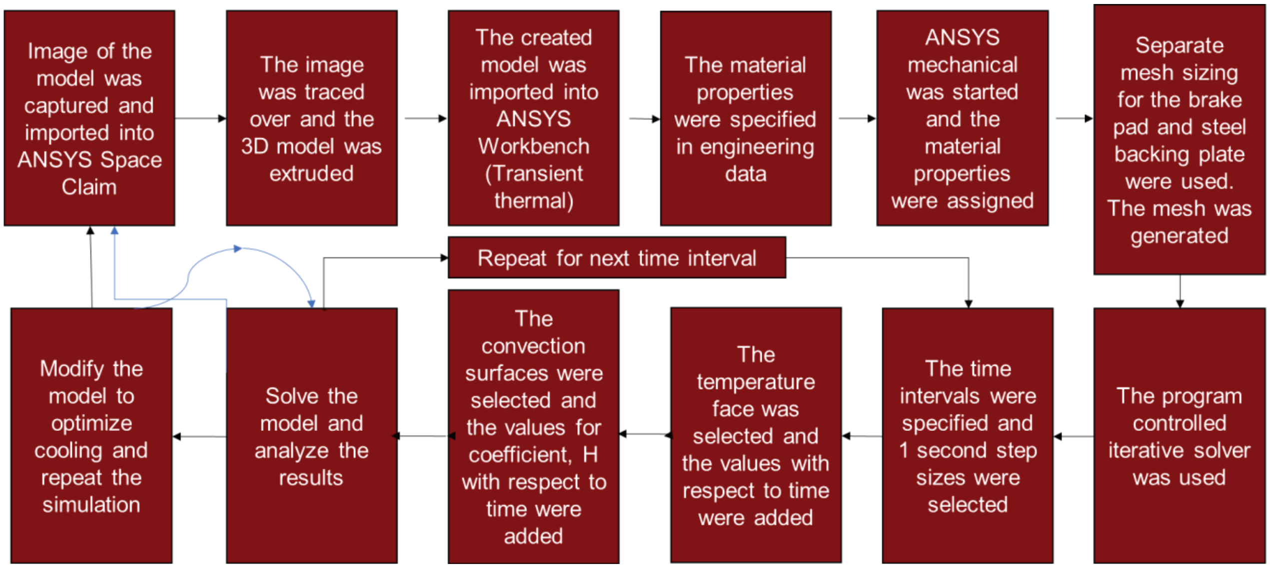

Figure 4.3.8: Finite Element Analysis Summary

4.4 TEST FOR FEA VALIDATION

Finite element analysis is an approximation method and never the final solution. As a result, it is imperative to develop tests to validate the FEA model. The following test was developed based on the parameters of this thesis study. The test includes instructions for the apparatus needed, the location for thermocouples to be placed on the brake pad, instructions for burnishing and instructions for the brake fade test

Apparatus:

- 1 Set Front Wagner Ford F-150 Brake pads
- 1 Set Front Power Stop Ford F-150 Brake pads
- 1 Set of front rotors for Ford F-150 for Wagner test
- 1 Set of front rotors for Ford F-150 for Power Stop test
- Stop watch
- 6 Thermocouples (6 for the front) (3 per pad x 2)
- Thermocouple data logger. Intervals set at 0.5 or 1 seconds
- Ford F-150

Wagner Locations

The thermocouples were placed in the location of the red circles in the image. A hole as deep as 1.2cm was drilled into the pad. Caution was exercised to not reach the friction material surface.

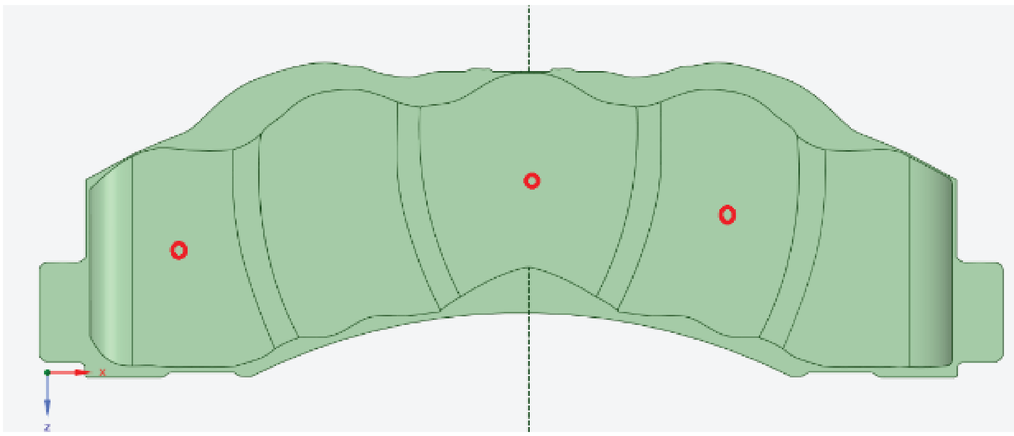

Figure 4.4: Wagner Thermocouple Locations (Front View)

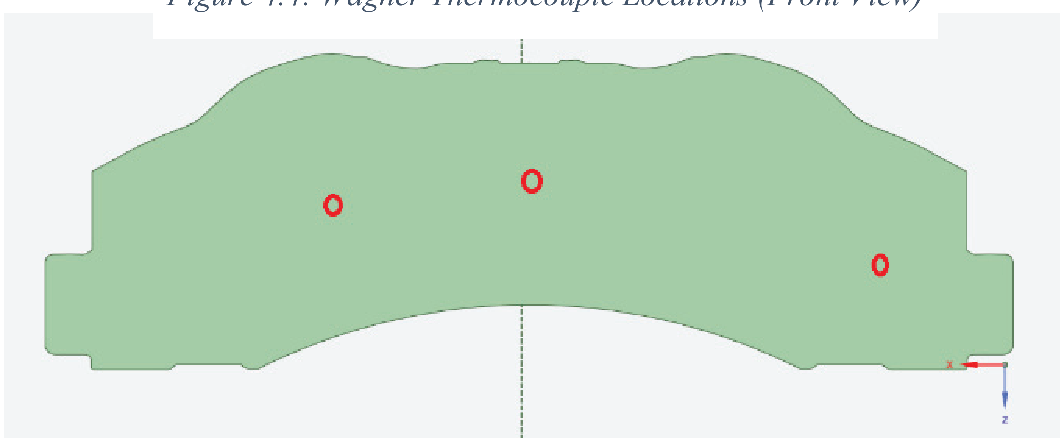

Figure 4. 5: Wagner Thermocouple Locations (Rear View)

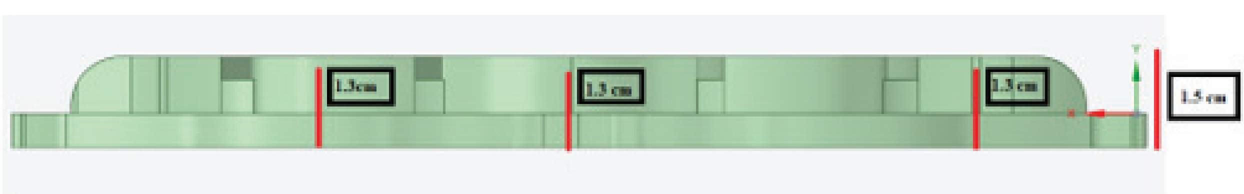

Figure 4. 6: Wagner Thermocouple Locations (Top View)

Power Stop Locations

The thermocouples were placed in the location of the red circles in the image. A hole as deep as 1.3cm for the 2 center locations and 0.8 cm for the side location were drilled.

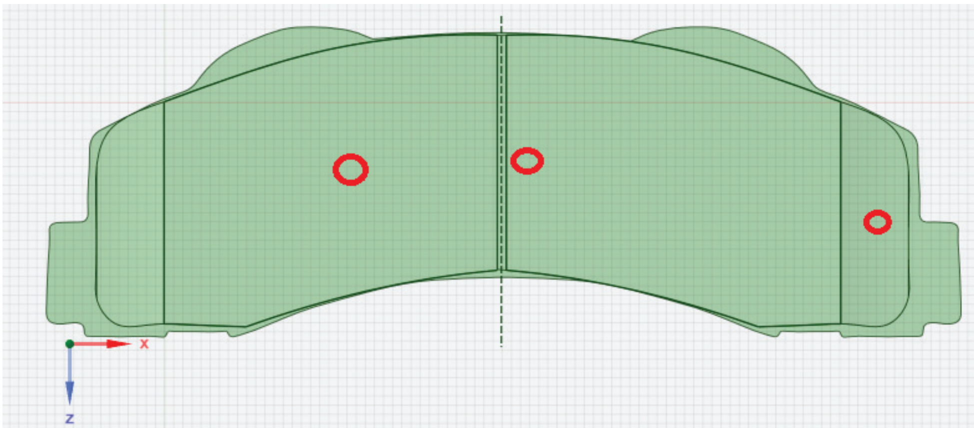

Figure 4. 7: Power Stop Thermocouple Locations (Front View)

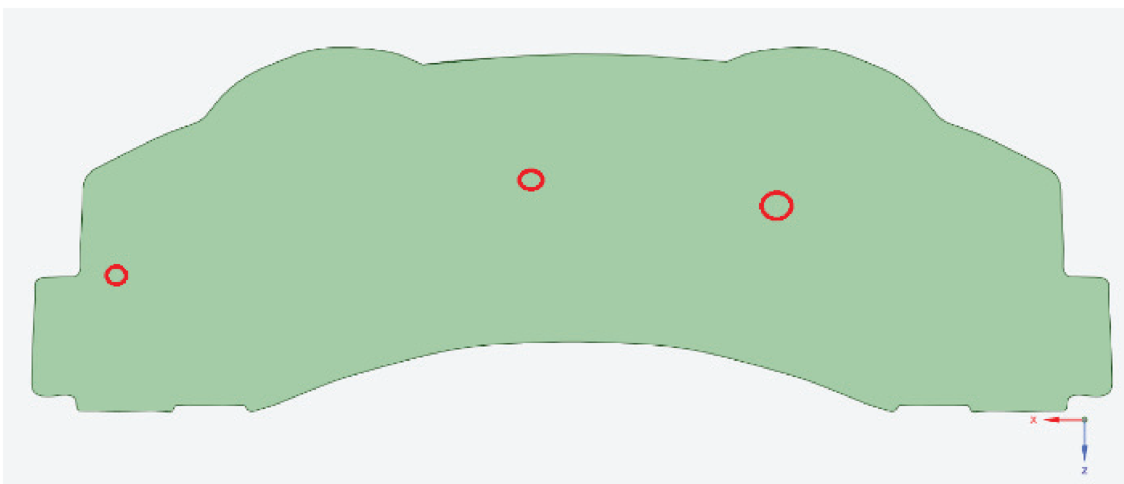

Figure 4. 8: Power Stop Thermocouple Locations (Rear View)

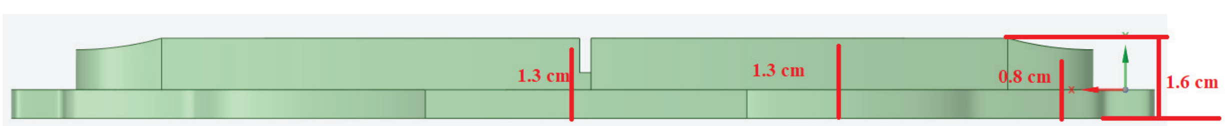

Figure 4. 9: Power Stop Thermocouple Locations (Top View)

Fade Stop Test

This involved getting the temperature of the brakes to about 550 °C.

Parameter	Front axle	Rear axle Disc brake	Rear axle Drum brake
Number of stops per cycle	15	15	15
Brake speed (km/h)	100	100	100
Release speed (km/h)	≤5	≤5	≤5
Deceleration level (g)	0.4	0.4	0.4
Maximum pressure (kPa)	16 000	16 000	10 000
Initial temperature 1 (°C)	≤100	≤100	≤100
Initial temperature 2 (°C)	≤215	≤215	≤151
Initial temperature 3 (°C)	≤283	≤283	≤181
Initial temperature 4 (°C)	≤330	≤330	≤202
Initial temperature 5 (°C)	≤367	≤367	≤219
Initial temperature 6 (°C)	≤398	≤398	≤232
Initial temperature 7 (°C)	≤423	≤423	≤244
Initial temperature 8 (°C)	≤446	≤446	≤254
Initial temperature 9 (°C)	≤465	≤465	≤262
Initial temperature 10 (°C)	≤483	≤483	≤270
Initial temperature 11 (°C)	≤498	≤498	≤277
Initial temperature 12 (°C)	≤513	≤513	≤284
Initial temperature 13 (°C)	≤526	≤526	≤289
Initial temperature 14 (°C)	≤539	≤539	≤295
Initial temperature 15 (°C)	≤550	≤550	≤300
Final brake temperature (°C)	Open	Open	Open
Number of cycles	1	1	1

Table 4.4.1: Fade Test

Deceleration of **0.4g from 100km/h to 5km/h takes 6.72 seconds**. This is the time the driver aimed for.

Fade Test instructions

Test from 100km/h to 5km/h (62 mph to 3mph) (6.72 seconds)

1) The driver accelerated to 100 km/h.
2) One 100 km/h was reached, the brakes were applied (Attempting to slow to 5km/h in 6.72 seconds).
3) The temperatures of the brake pads were logged in the data logger.
4) This test was repeated until brake fade temperatures of over 500 ºC.

CHAPTER 5 - RESULTS

5.1 RESULTS

It must be said that the conduction heat transfer between the brake pad and the disk also accounts for a large portion of the heat transfer. If the materials in either pad have higher thermal conductivities, there is a possibility that the other brake pads will cool faster. Brake rotors also play a huge role in absorbing heat. This study is solely considering the effect of convective cooling. Well over 20 models have been developed and simulations ran. The results include the 2 designs that are the most feasible to machine. The results section consists of 4 brake pads. The original Wagner [26] brake pad, the original PowerStop brake pad, a PowerStop pad modified with slots on the friction material and a power stop model modified with slots and wavy features on the top of the pad.

Brake Fade Test

Many different simulations could be performed to determine the change in temperature during the braking process. The aim of this study was to determine the role convective cooling played in decreasing the brake pad temperature. For this specific application, the brake fade test is determined to be the most applicable. The brakes are engaged and disengaged 7 times in 105s and allowed to cool with the vehicle moving at around 60 km/h until 150s. Calculations are based on kinetic energy of the vehicle. These calculations can be seen in chapter 4.

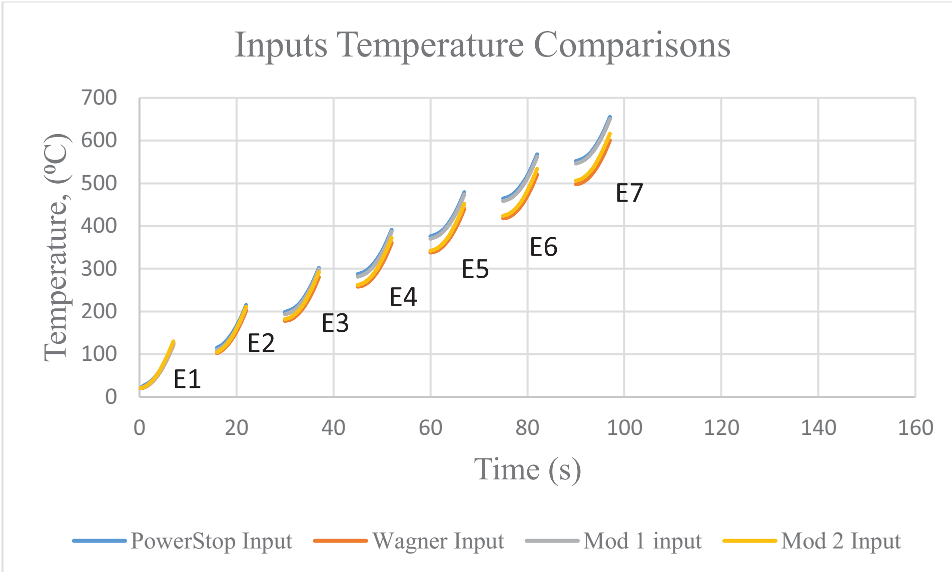

Figure 5.1.1: Comparison between input temperatures over time for the Wagner, Power Stop, Power Stop Mod 1 and Power Stop Mod 2 brake pads

As can be seen in figure 5.1.1, for the first few engagements the temperatures do not stray far from each other, however around the 4th engagement, the Wagner brake pads and the 2nd modified Power Stop brake pad begin to show the effect of the convective slots and waves.

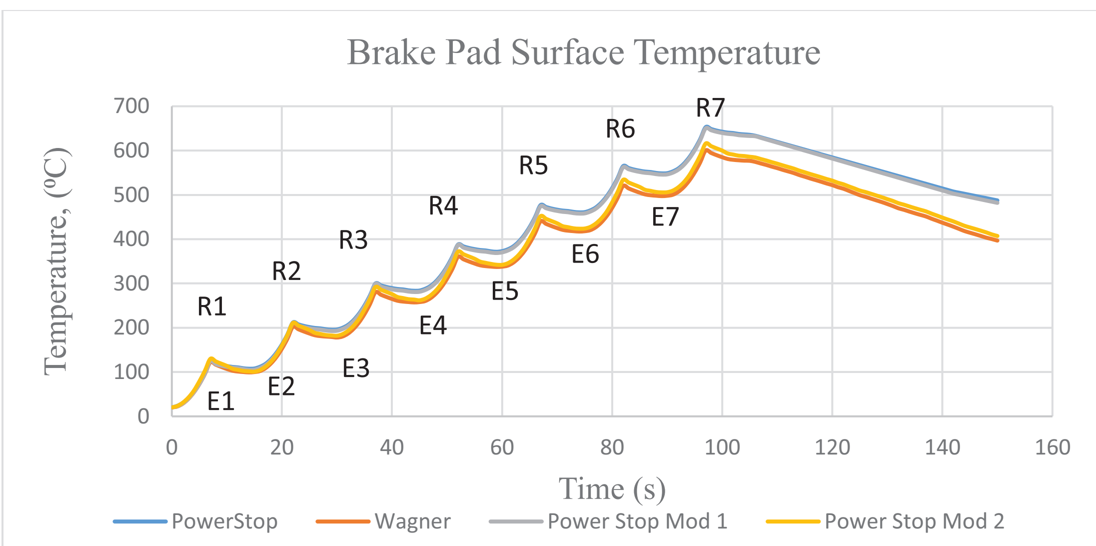

Figure 5.1.2: Graph of the surface temperature over time for the Wagner, Power Stop, Power Stop Mod 1 and Power Stop Mod 2 brake pads

Figure 5.1.2 is the overall maximum temperatures on the face of the brake pad friction material. The effect of the slots on the Power stop mod 1 brake pad is almost negligible. The heating on the Wagner [26] brake pad is the lowest compared to the rest. This can be attributed to the mass of the brake pad being slightly higher than the power stop brake pad. At release 2 a gap in performance can be seen between the original Power Stop, the Power stop mod 1 brake pad and the Wagner [26] and, Power Stop Mod 2 brake pad, this can be attributed to the convective cooling due to turbulent airflow in the peaks, valleys and slots.

5.2 WAGNER BRAKE PAD

This is the model of the original Wagner [26] Brake Pad. The analysis of this brake pad was used as the benchmark of this study.

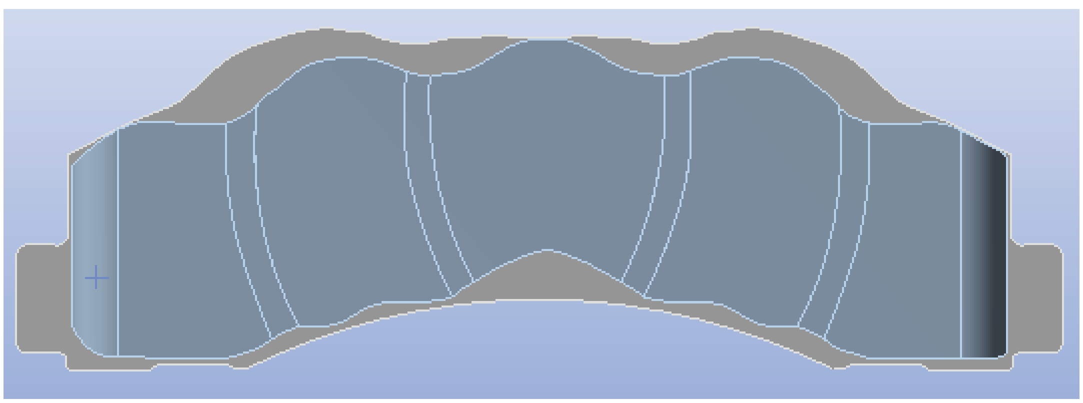

Figure 5.2.1: Model of Wagner brake pad

For this pad, the wavy figures along with the slots that run from the top to the bottom of the friction material on the pad, contributed significantly to the convective cooling of the brake pad. The values that were input for the simulations were initial temperature and convection heat transfer coefficient. The temperatures and heat transfer coefficients are calculated as described in chapter 4.

Table 5.2.1: Wagner Convective heat transfer values between 20ºC - 100ºC

				Over all			Slots			Rounded Peaks		
Density	Dynamic Viscosity	Conductivity	Prandlt	ReyNolds	Nu	h	ReyNolds	Nu	h	ReyNolds	Nu	h
1.164	0.00001872	0.02588	0.7282	6.57E+05	484.06	32.967	2.80E+04	99.978	64.686	2.10E+04	86.583	74.69267
1.164	0.00001872	0.02588	0.7282	5.56E+05	445.48	30.34	2.37E+04	92.01	59.531	1.78E+04	79.683	68.74001
1.164	0.00001872	0.02588	0.7282	4.59E+05	404.79	27.568	1.96E+04	83.605	54.093	1.47E+04	72.404	62.46074
1.164	0.00001872	0.02588	0.7282	3.65E+05	360.73	24.568	1.56E+04	74.505	48.205	1.17E+04	64.524	55.66238
1.092	0.00001963	0.02735	0.7228	2.43E+05	293.76	21.143	1.04E+04	60.674	41.486	7.78E+03	52.545	47.90378
1.092	0.00001963	0.02735	0.7228	1.60E+05	238.66	17.178	6.85E+03	49.294	33.705	5.13E+03	42.69	38.91901
1.092	0.00001963	0.02735	0.7228	7.77E+04	166.04	11.95	3.31E+03	34.293	23.448	2.48E+03	29.699	27.07547
0.9994	0.00002096	0.02953	0.7154	1.29E+04	67.304	5.2303	5.48E+02	13.901	10.263	4.11E+02	12.039	11.85012
0.9994	0.00002096	0.02953	0.7154	12850.2579	67.304	5.2303	548.1827483	13.901	10.263	411.137	12.039	11.85012
0.9994	0.00002096	0.02953	0.7154	8.23E+04	170.28	13.233	3.51E+03	35.17	25.965	2.63E+03	30.458	29.9813
0.9994	0.00002096	0.02953	0.7154	1.51E+05	230.76	17.932	6.44E+03	47.661	35.186	4.83E+03	41.275	40.62883
0.9994	0.00002096	0.02953	0.7154	2.19E+05	277.62	21.574	9.33E+03	57.341	42.332	7.00E+03	49.659	48.88053
0.9994	0.00002096	0.02953	0.7154	2.84E+05	316.68	24.609	1.21E+04	65.407	48.287	9.10E+03	56.644	55.75671
0.9994	0.00002096	0.02953	0.7154	3.48E+05	350.31	27.223	1.49E+04	72.354	53.416	1.11E+04	62.661	61.67914
0.9994	0.00002096	0.02953	0.7154	4.09E+05	379.82	29.516	1.75E+04	78.448	57.914	1.31E+04	67.938	66.87341
0.9994	0.00002096	0.02953	0.7154	4.68E+05	405.98	31.549	1.99E+04	83.852	61.904	1.50E+04	72.618	71.4801
0.9994	0.00002096	0.02953	0.7154	5.23E+05	429.36	33.366	2.23E+04	88.681	65.469	1.67E+04	76.8	75.59654

Table 5.2.2: Wagner initial FEA inputs, time = 0s to 15s

time(s)	Temperatures	Convective Over All	Convective Slots	Rounded Peaks
0	20	32.96691014	64.68574867	74.69266882
1	25.134	30.33959867	59.53059133	68.74000586
2	31.482	27.5681332	54.09258339	62.46073516
3	41.771	24.56756057	48.20503475	55.66237958
4	56.645	21.1431678	41.48589094	47.9037806
5	74.997	17.17758297	33.70485164	38.91901033
6	98.097	11.95023237	23.44804911	27.07547493
7	124.83	5.230259015	10.26250925	11.85012495
8	[redacted]	5.230259015	10.26250925	11.85012495
9	[redacted]	13.23276952	25.96456871	29.98130147
10	[redacted]	17.93224114	35.18559788	40.62882881
11	[redacted]	21.57427317	42.33178075	48.88053003
12	[redacted]	24.60919518	48.28672774	55.75671052
13	[redacted]	27.22316114	53.41569933	61.67913678
14	[redacted]	29.51574227	57.91406832	66.87340587
15	[redacted]	31.54898892	61.90358634	71.48010448

Table 5.2.1 show the respective density, dynamic viscosity, thermal conductivity, Prandtl number, calculations for the Reynolds number, Nusselt's number and finally the convective heat

transfer coefficient for the Wagner Pad. These values change over time as well as temperature, further tables are included in the appendix.

Table 5.2.2 is the values that are input into ANSYS [24], at time = 8 (s) the heating is stopped while the convective heat transfer coefficient remains in effect until time = 15 (s). At t = 15(s) the brakes are then engaged again, and the heat is the applied to for 7 seconds (100 km/h to 5km/h) and the cycle then continues.

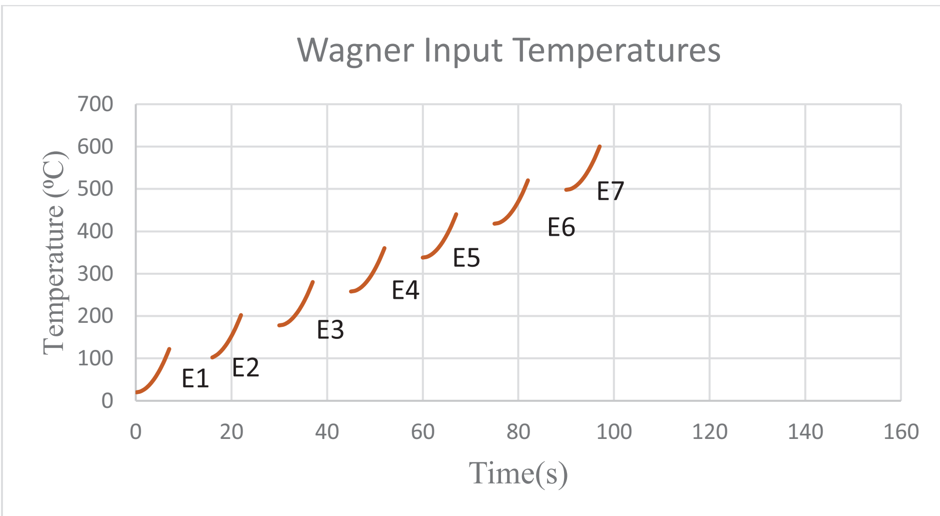

Figure 5.2.2: Summary of Wagner temperature inputs

The finite element analysis temperatures that were input is summarized in Figure 5.2.2. The values are provided in the appendix. Heat is initially applied for 7 seconds, allowed to cool for 8 seconds (for the vehicle to get up to speed) and then applied again. This is repeated until brake fade temperatures of above 550 ºC are reached.

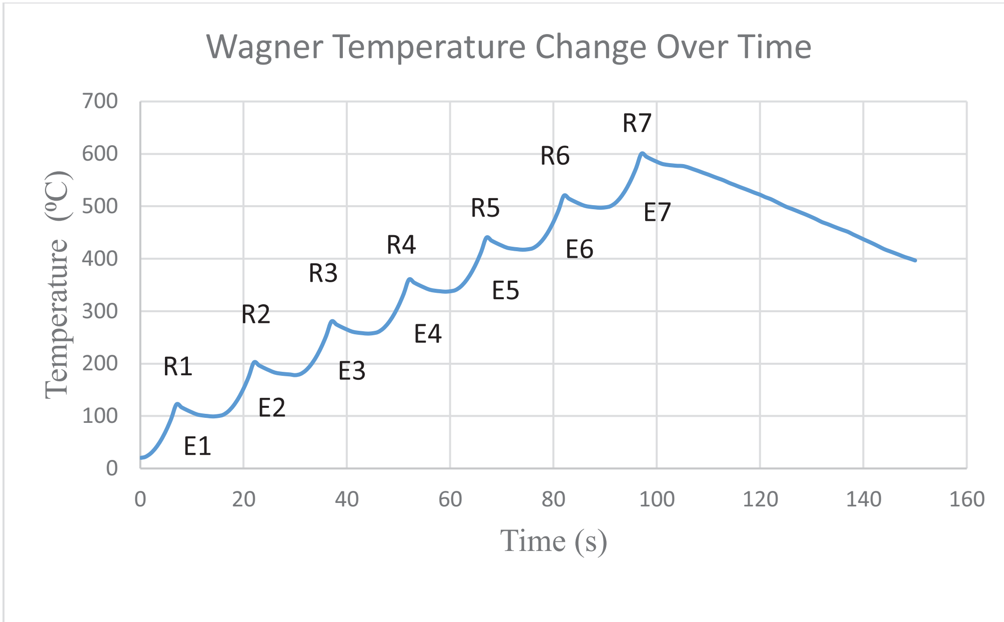

Figure 5.2.3: Temperature change for Wagner brake pad over Time

The ambient temperature is 20ºC and on average each engagement raises the average temperature by 102 ºC. While the vehicle is then brought up to speed the pad loses an average of about 20 - 25 ºC in 8 seconds. After 7 repeated engagements, each engagement with an interval of 15 seconds brake fade is seen to start at time = 82s, however it the cools below 500ºC quickly after. The next and final engagement brings the maximum temperature to around 600 ºC. The heat is then no longer applied and the brake can cool until t=150(s), the temperature at this time is 396 ºC.

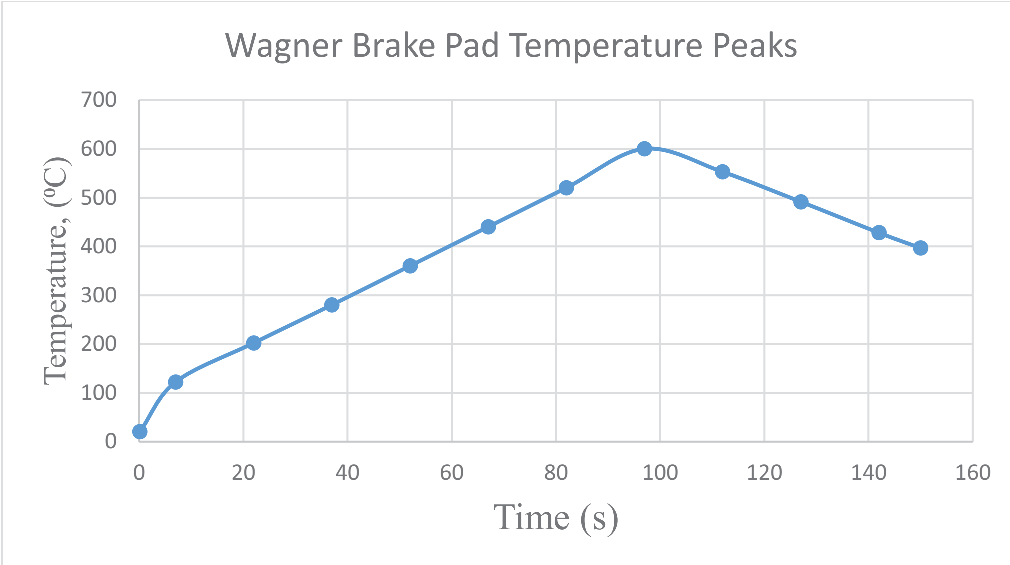

Figure 5.2.4 Temperature peaks for Wagner brake pad

Figure 5.2.4 shows the maximum temperature of each engagement with respect to time. This is a clear visualization of how the pad increases and decreases in temperature over 150 seconds.

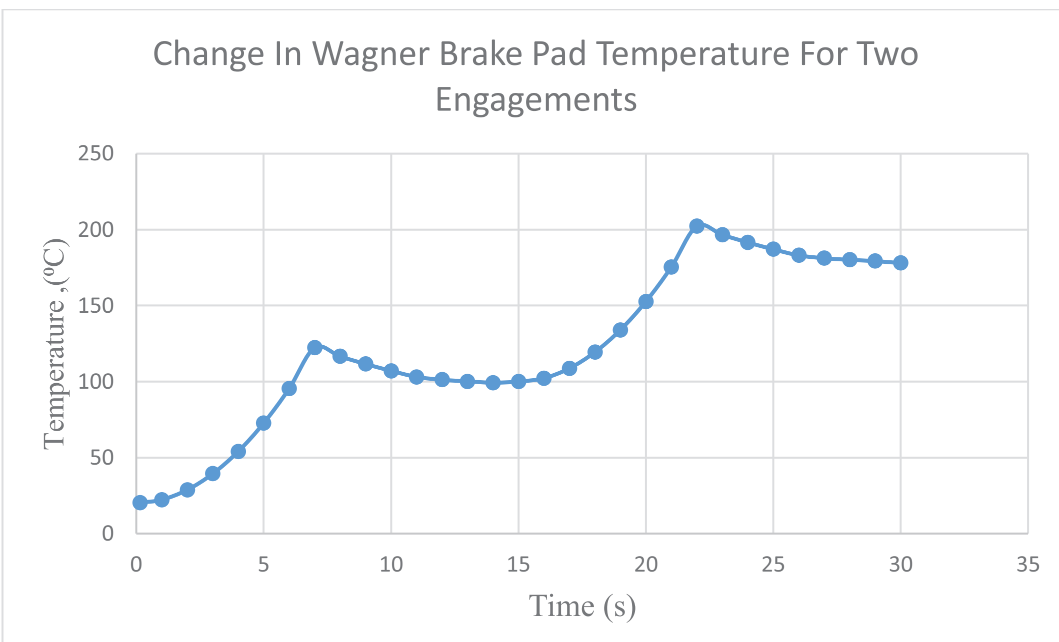

Figure 5.2.5: Wagner Temperature change for 2 engagements

Figure 5.2.5 details the change in temperature with respect to time. An average of a 20 - 25ºC drop can be seen prior to the next brake engagement. This trend is generally followed throughout the simulation.

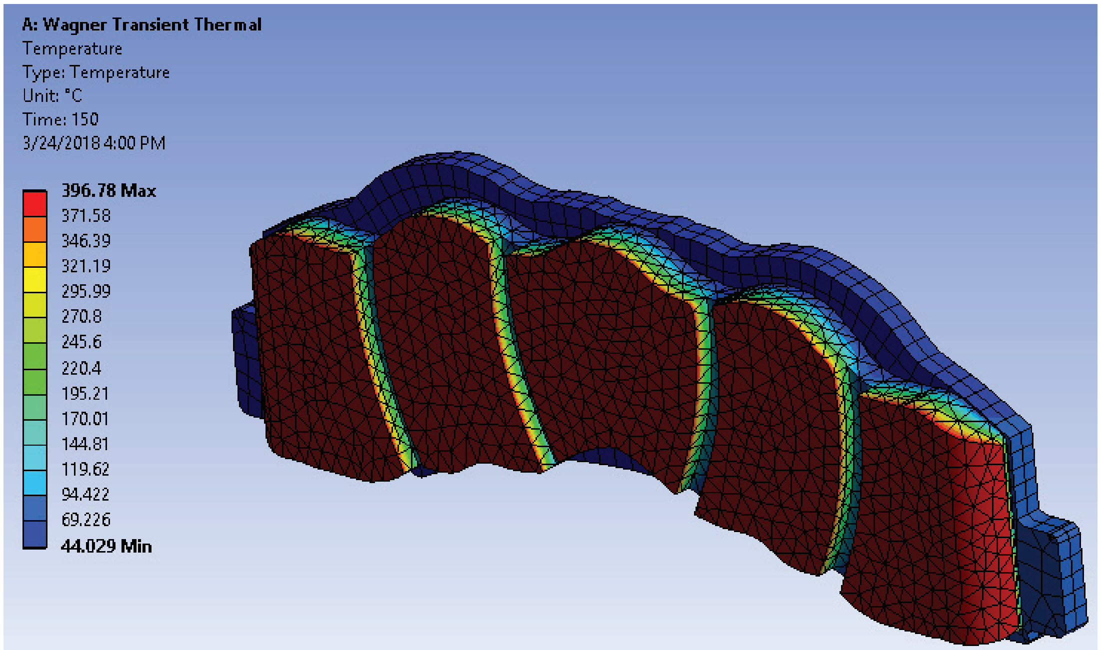

Figure 5.2.6: Wagner Model final temperature gradient

5.3 POWER STOP BRAKE PAD

This is the model of the original Power Stop Brake pad. The analysis of this brake pad was used as the benchmark of this study. This brake pad design was then also modified for better convective cooling.

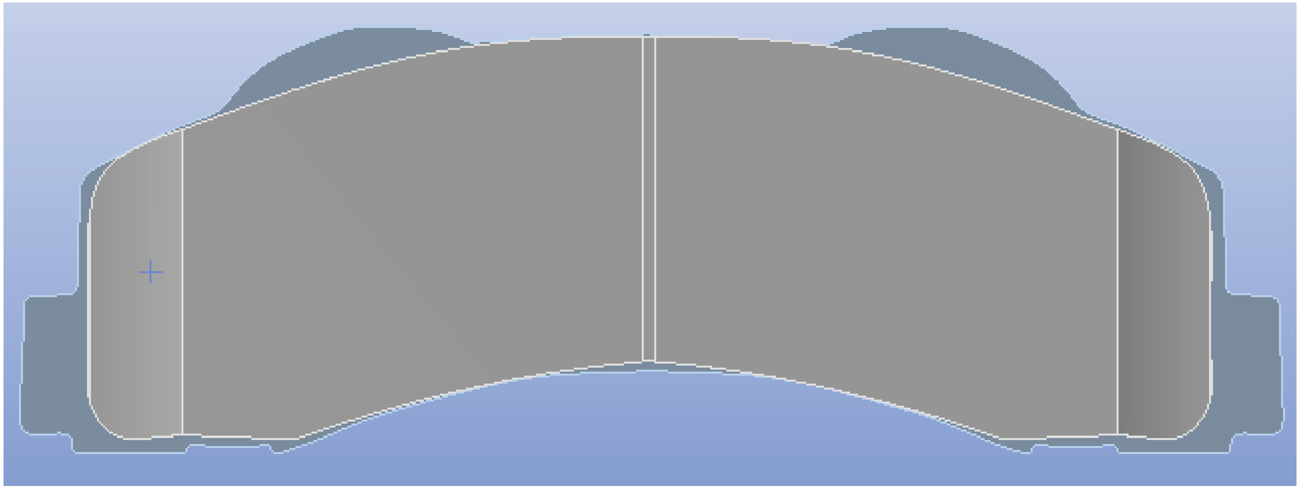

Figure 5.3.1: Model of Power Stop brake pad

This brake pad does not have features that promote turbulent airflow, when compared to the Wagner brake pad [26]. As calculations have shown, the use of peaks and valleys as well as slots running from the top of the brake pad friction material increase the convective heat transfer coefficient of the surface in contact with the fluid. In comparison to the Wagner pad [26], the slot in the center only provides a maximum heat transfer coefficient of 6.09 W/m2 ºC, compared to the Wagner pad [26] at 64 W/m2 ºC.

Table 5.3.1: Power Stop convective heat transfer values < 100ºC

				Over all			Slots			Rounded Peaks		
Density	Dynamic Viscosity	Conductivity	Prandlt	ReyNolds	Nu	h	ReyNolds	Nu	h	ReyNolds	Nu	h
1.164	0.00001872	0.02588	0.7282	6.57E+05	484.06	32.96691014	3.50E+03	35.348	6.098630871	1.05E+05	193.61	33.40358
1.164	0.00001872	0.02588	0.7282	5.56E+05	445.48	30.33959867	2.97E+03	32.531	5.612597975	8.90E+04	178.18	30.74147
1.164	0.00001872	0.02588	0.7282	4.59E+05	404.79	27.5681332	2.45E+03	29.559	5.09989767	7.35E+04	161.9	27.93329
1.164	0.00001872	0.02588	0.7282	3.65E+05	360.73	24.56756057	1.95E+03	26.342	4.544814261	5.84E+04	144.28	24.89297
1.092	0.00001963	0.02735	0.7228	2.43E+05	293.76	21.1431678	1.30E+03	21.452	3.911327307	3.89E+04	117.49	21.42322
1.092	0.00001963	0.02735	0.7228	1.60E+05	238.66	17.17758297	8.56E+02	17.428	3.177723887	2.57E+04	95.458	17.40511
1.092	0.00001963	0.02735	0.7228	7.77E+04	166.04	11.95023237	4.14E+02	12.125	2.210703271	1.24E+04	66.409	12.10852
0.9994	0.00002096	0.02953	0.7154	1.29E+04	67.304	5.230259015	6.85E+01	4.9148	0.967558651	2.06E+03	26.919	5.299537
0.9994	0.00002096	0.02953	7.15E-01	12850.2579	67.304	5.23E+00	68.52284353	4.9148	9.68E-01	2055.6853	26.919	5.299537
0.9994	0.00002096	0.02953	0.7154	8.23E+04	170.28	13.23276952	4.39E+02	12.435	2.447963014	1.32E+04	68.107	13.40805
0.9994	0.00002096	0.02953	0.7154	1.51E+05	230.76	17.93224114	8.05E+02	16.851	3.317329981	2.42E+04	92.295	18.16976
0.9994	0.00002096	0.02953	0.7154	2.19E+05	277.62	21.57427317	1.17E+03	20.273	3.991078564	3.50E+04	111.04	21.86004
0.9994	0.00002096	0.02953	0.7154	2.84E+05	316.68	24.60919518	1.52E+03	23.125	4.552516351	4.55E+04	126.66	24.93516
0.9994	0.00002096	0.02953	0.7154	3.48E+05	350.31	27.22316114	1.86E+03	25.581	5.036080429	5.57E+04	140.11	27.58375
0.9994	0.00002096	0.02953	0.7154	4.09E+05	379.82	29.51574227	2.18E+03	27.735	5.460190725	6.55E+04	151.91	29.9067
0.9994	0.00002096	0.02953	0.7154	4.68E+05	405.98	31.54898892	2.49E+03	29.646	5.836326091	7.48E+04	162.38	31.96687
0.9994	0.00002096	0.02953	0.7154	5.23E+05	429.36	33.3658495	2.79E+03	31.353	6.172431659	8.37E+04	171.73	33.8078

Table 5.3.2: Power Stop Initial FEA inputs, Time = 0(s) to 15(s)

time(s)	Temperatures	Convective Over All	Convective Slots	Rounded Peaks
0	20	32.96691014	6.098630871	33.40357698
1	26.964	30.33959867	5.612597975	30.74146517
2	33.262	27.5681332	5.09989767	27.93328995
3	43.721	24.56756057	4.544814261	24.89297291
4	58.035	21.1431678	3.911327307	21.42322196
5	76.917	17.17758297	3.177723887	17.40511054
6	99.337	11.95023237	2.210703271	12.10852049
7	126.64	5.230259015	0.967558651	5.299536988
8		5.230259015	0.967558651	5.299536988
9		13.23276952	2.447963014	13.40804563
10		17.93224114	3.317329981	18.16976461
11		21.57427317	3.991078564	21.86003758
12		24.60919518	4.552516351	24.93515899
13		27.22316114	5.036080429	27.58374853
14		29.51574227	5.460190725	29.90669628
15		31.54898892	5.836326091	31.96687453

Table 5.3.1 shows the respective density, dynamic viscosity, thermal conductivity, Prandtl number, calculations for the Reynolds number, Nusselt's number and finally the convective heat transfer coefficient for the PowerStop pad. These values change over time as well as temperature, further tables are included in the appendix.

Table 5.3.2 are the values that are input into ANSYS [24], at time = 8 s the heating is stopped while the convective heat transfer coefficient remains in effect until time = 15 (s). At t = 15(s) the brakes are then engaged again, and the heat is the applied to for 7 seconds (100 km/h to 5km/h) and the cycle then continues.

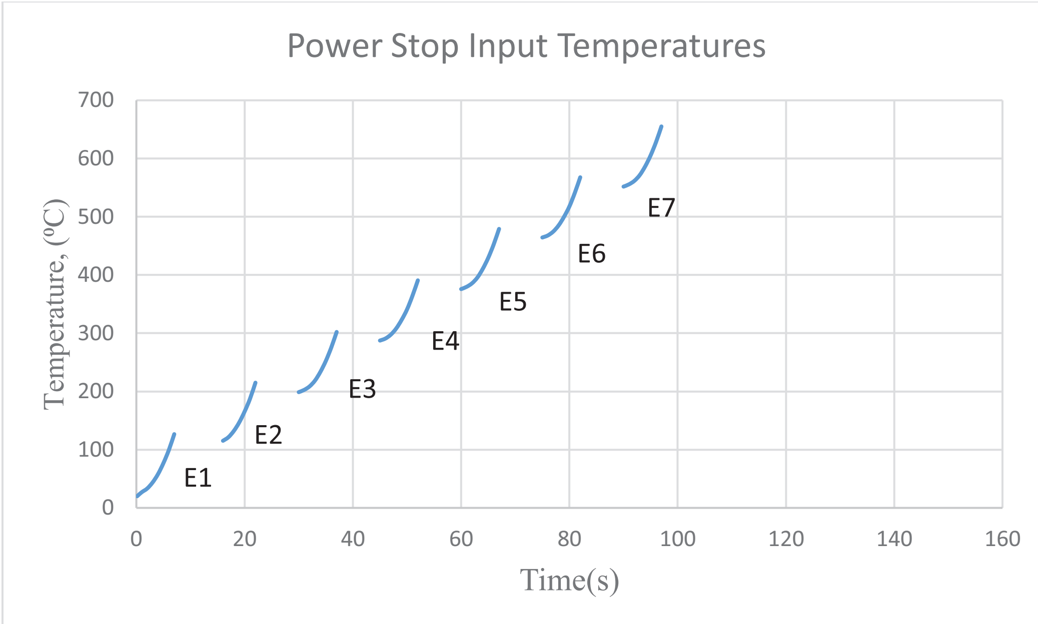

Figure 5.3.2: Summary of Power Stop inputs

The finite element analysis temperatures that were input into ANSYS [24] for the Power Stop brake pad is summarized in Figure 5.3.2. The values are provided in the appendix. Heat is initially applied for 7 seconds, allowed to cool for 8 seconds (for the vehicle to get up to speed) and then applied again. This is repeated until brake fade temperatures of above 550 ºC are reached.

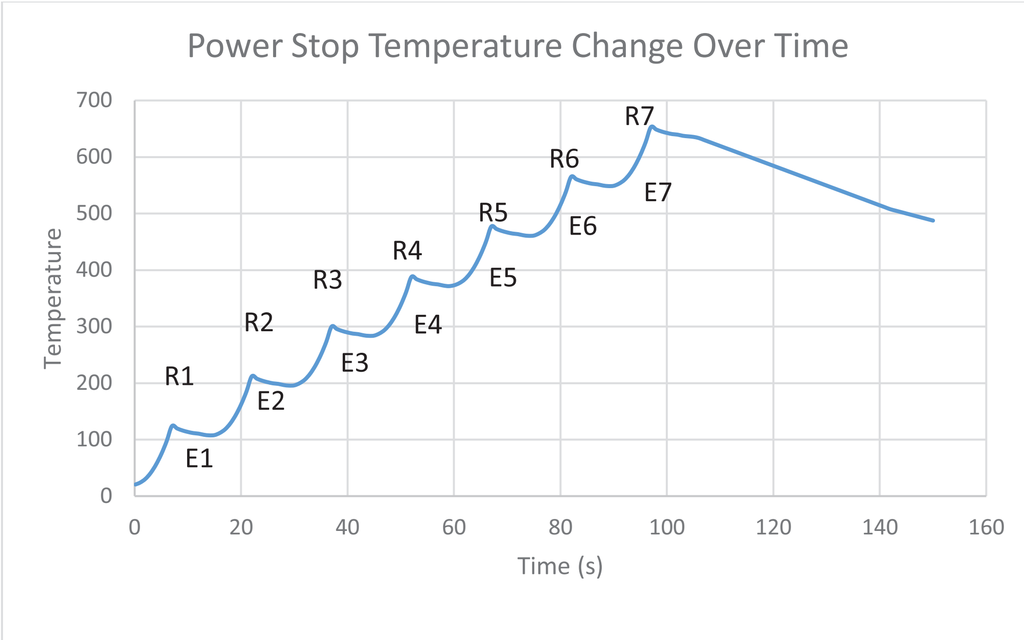

Figure 5.3.3: Temperature change for Power Stop brake pad over Time

The ambient temperature is 20ºC and on average each engagement raises the average temperature by 106.64 ºC. While the vehicle is then brought up to speed the pad loses an average of about 10 - 15 ºC in 8 seconds. After 7 repeated engagements, each engagement with an interval of 15 seconds, brake fade is seen to start at time = 82 s, where the temperature is 567 ºC. It then cools to 548 ºC during the 8 second interval. The next and final engagement brings the maximum temperature to around 655 ºC. The heat is then no longer applied and the brake can cool until t=150(s), the temperature now is 487.5 ºC. The values for this chart is provided in the appendix.

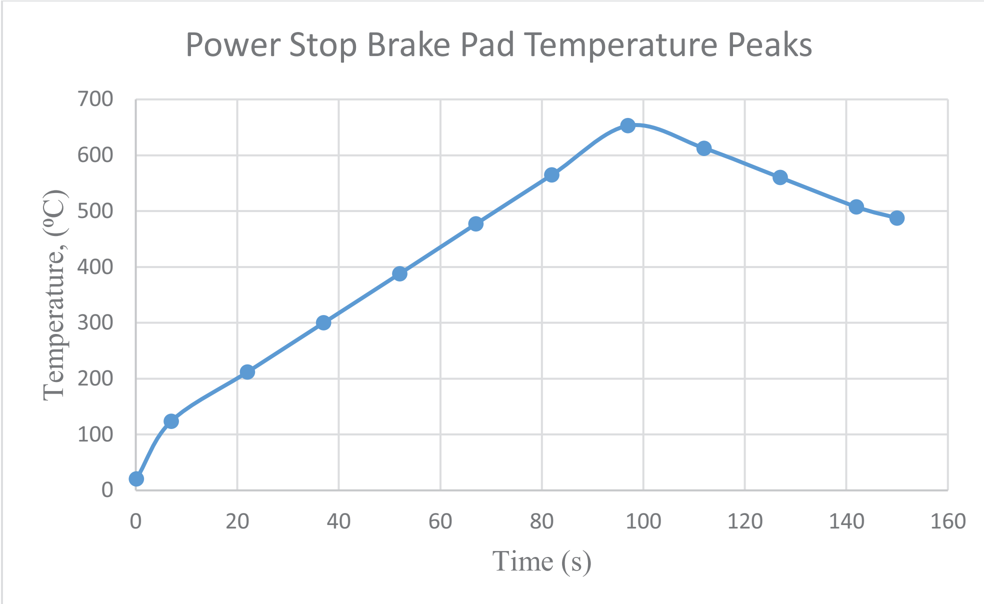

Figure 5.3.4: Temperature peaks for Power Stop Brake Pads

Figure 5.3.4 shows the maximum temperature of each engagement with respect to time. This is a clear visualization of how the pad increases and decreases in temperature over 150 seconds.

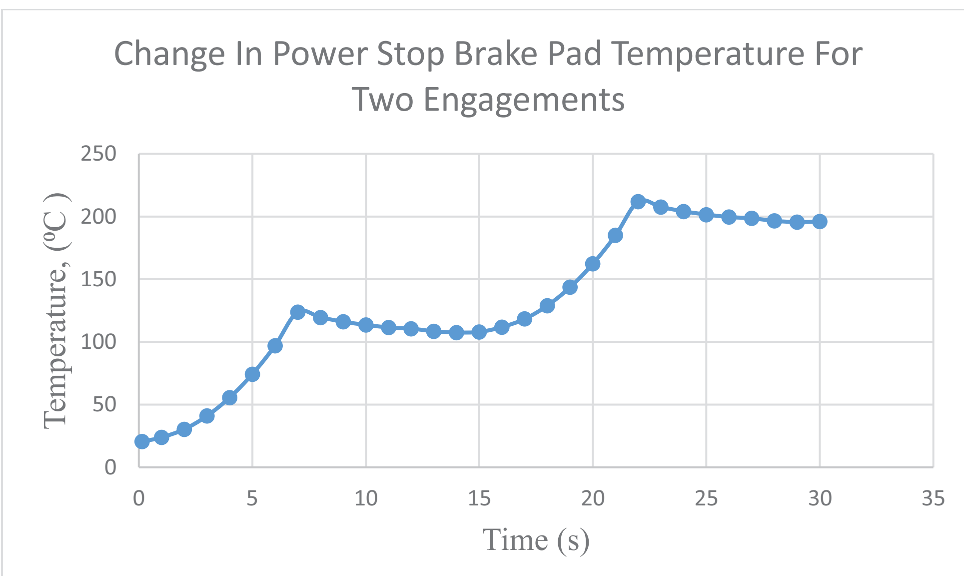

Figure 5.3.5: Power Stop temperature change for 2 engagements

Figure 5.3.5 details the change in temperature with respect to time. An average of a 10 - 15ºC drop can be seen prior to the next brake engagement. This trend is generally followed throughout the simulation.

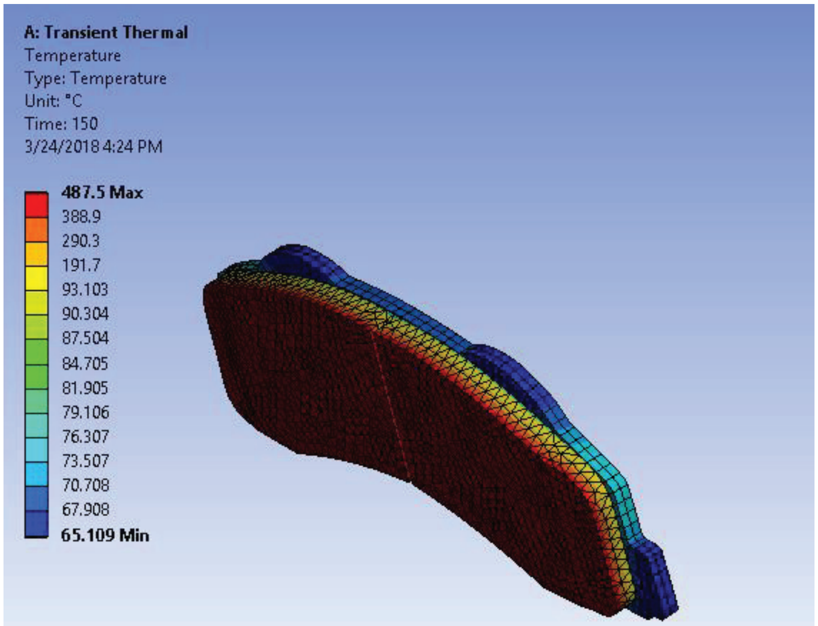

Figure 5.3.6: Power Stop model final temperature gradient

5.4 MODIFIED POWER STOP MODEL WITH STRAIGHT SLOTS

This is the model of the modified power stop brake pad. The original power stop pad was modified and slots were added to determine if there was any significant impact to the overall cooling of the brake pad.

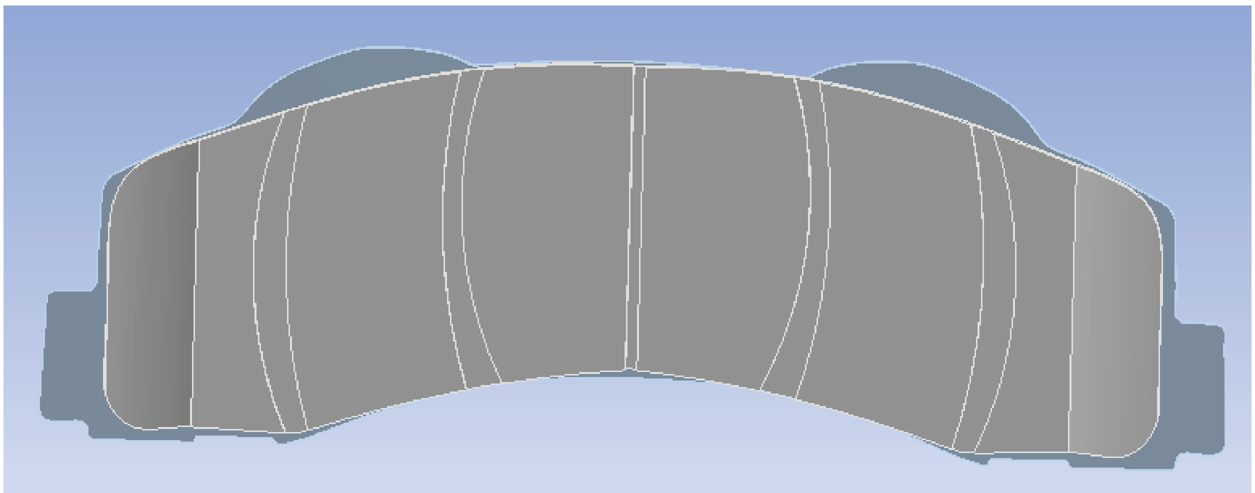

Figure 5.4. 1: Modified Power Stop Brake Pad

For this pad, the slots that run from the top to the bottom of the friction material on the pad did contribute to the overall cooling of the brake pad. While the temperatures were slightly cooler, the temperatures were within a 2 – 3 % difference from the original PowerStop brake pad. Based on this it can be determine that the rounded peaks on the friction material of the pad make a big difference the values that were input for the simulations were initial temperature and convection heat transfer coefficient. The temperatures and heat transfer coefficients are calculated as described in chapter 4.

Table 5.4.1: Modified power stop pad 1 convective heat transfer values <100ºC

				Over all			Slots			Rounded Peaks		
Density	Dynamic Viscosity	Conductivity	Prandlt	ReyNolds	Nu	h	ReyNolds	Nu	h	ReyNolds	Nu	h
1.164	0.00001872	0.02588	0.7282	6.57E+05	484.06	32.967	3.85E+04	117.23	20.227	1.08E+05	196.17	32.96691
1.164	0.00001872	0.02588	0.7282	5.56E+05	445.48	30.34	3.26E+04	107.89	18.615	9.14E+04	180.54	30.3396
1.164	0.00001872	0.02588	0.7282	4.59E+05	404.79	27.568	2.69E+04	98.036	16.914	7.54E+04	164.05	27.56813
1.164	0.00001872	0.02588	0.7282	3.65E+05	360.73	24.568	2.14E+04	87.365	15.073	5.99E+04	146.19	24.56756
1.092	0.00001963	0.02735	0.7228	2.43E+05	293.76	21.143	1.43E+04	71.147	12.972	3.99E+04	119.05	21.14317
1.092	0.00001963	0.02735	0.7228	1.60E+05	238.66	17.178	9.41E+03	57.802	10.539	2.64E+04	96.722	17.17758
1.092	0.00001963	0.02735	0.7228	7.77E+04	166.04	11.95	4.56E+03	40.212	7.3321	1.28E+04	67.288	11.95023
0.9994	0.00002096	0.02953	0.7154	1.29E+04	67.304	5.2303	7.54E+02	16.301	3.209	2.11E+03	27.276	5.230259
0.9994	0.00002096	0.02953	0.7154	12850.2579	67.304	5.2303	753.7512789	16.301	3.209	2110.5	27.276	5.230259
0.9994	0.00002096	0.02953	0.7154	82255.8791	170.28	13.233	4824.842769	41.241	8.119	13509.6	69.009	13.23277
0.9994	0.00002096	0.02953	0.7154	151054.821	230.76	17.932	8860.348599	55.887	11.002	24809	93.517	17.93224
0.9994	0.00002096	0.02953	0.7154	218644.118	277.62	21.574	12824.90082	67.238	13.237	35909.7	112.51	21.57427
0.9994	0.00002096	0.02953	0.7154	284485.59	316.68	24.609	16686.93176	76.697	15.099	46723.4	128.34	24.6092
0.9994	0.00002096	0.02953	0.7154	348130.889	350.31	27.223	20420.14287	84.843	16.703	57176.4	141.97	27.22316
0.9994	0.00002096	0.02953	0.7154	409235.095	379.82	29.516	24004.30229	91.988	18.109	67212	153.93	29.51574
0.9994	0.00002096	0.02953	0.7154	467558.915	405.98	31.549	27425.37406	98.325	19.357	76791	164.53	31.54899
0.9994	0.00002096	0.02953	0.7154	522961.629	429.36	33.366	30675.10385	103.99	20.472	85890.3	174	33.36585

Table 5.4.2: Modified power stop pad 1 Initial FEA inputs, Time = 0(s) to 15(s)

time(s)	Temperatures	Convective Over All	Convective Slots	Rounded Peaks
0	20	32.96691014	20.22687033	32.96691014
1	27.814	30.33959867	18.61488158	30.33959867
2	33.412	27.5681332	16.91444704	27.5681332
3	43.271	24.56756057	15.07344365	24.56756057
4	58.605	21.1431678	12.97240511	21.1431678
5	78.367	17.17758297	10.53931782	17.17758297
6	100.007	11.95023237	7.332073272	11.95023237
7	128.08	5.230259015	3.209029007	5.230259015
8		5.230259015	3.209029007	5.230259015
9		13.23276952	8.118974819	13.23276952
10		17.93224114	11.00233885	17.93224114
11		21.57427317	13.23691011	21.57427317
12		24.60919518	15.09898859	24.60919518
13		27.22316114	16.7027892	27.22316114
14		29.51574227	18.10940392	29.51574227
15		31.54898892	19.3569038	31.54898892

Table 5.4.1 show the respective density, dynamic viscosity, thermal conductivity, Prandtl number, calculations for the Reynolds number, Nusselt's number and finally the convective heat

transfer coefficient for the modified Power Stop 1 pad. These values change over time as well as temperature, further tables are included in the appendix.

Table 5.4.2 is the values that are input into ANSYS [24], at time = 8 (s) the heating is stopped while the convective heat transfer coefficient remains in effect until time = 15 (s). At t = 15(s) the brakes are then engaged again, and the heat is the applied to for 7 seconds (100 km/h to 5km/h) and the cycle then continues.

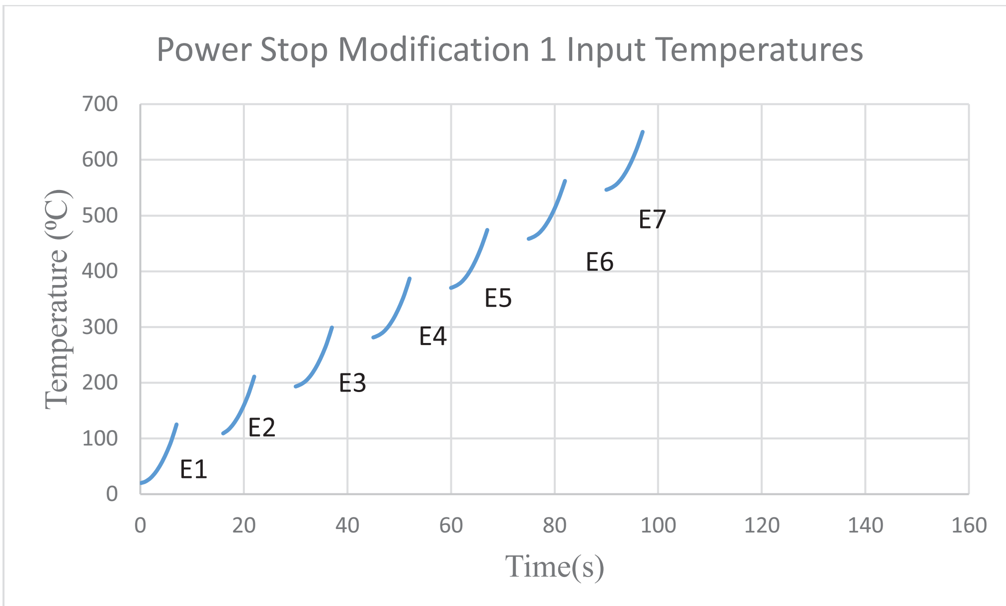

Figure 5.4.2: Summary of Power Stop modification 1 temperature inputs

The finite element analysis temperatures that were input into ANSYS [24] for the modified Power Stop brake pad is summarized in Figure 5.4.2. The values are provided in the appendix. Heat is initially applied for 7 seconds, allowed to cool for 8 seconds (for the vehicle to get up to speed) and then applied again. This is repeated until brake fade temperatures of above 550 ºC are reached.

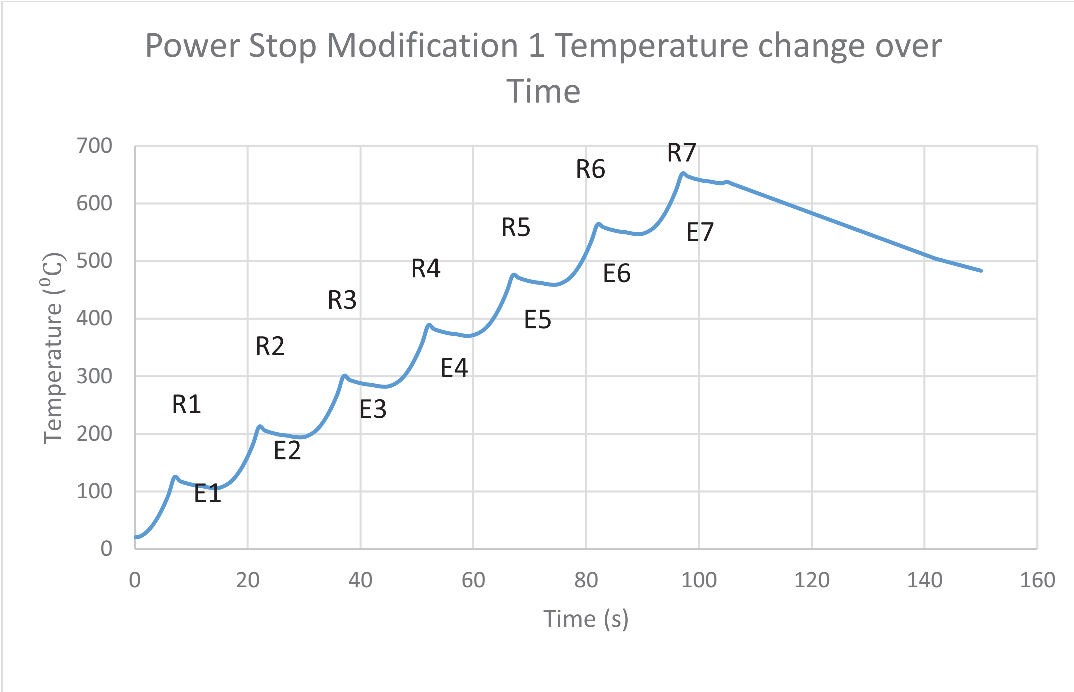

Figure 5.4.3: Temperature change for Power Stop Modification 1 brake pad over time

The ambient temperature is 20ºC and on average each engagement raises the average temperature by 128.08 ºC. This increase is even larger than the original power stop brake pad. This is because the when the slots are cut into the pad, the mass of the pad decreases. Based on the caloric heat equation, the change in temperature becomes larger. While the vehicle is then brought up to speed the pad loses an average of about 10-15 ºC in 8 seconds. After 7 repeated engagements, each engagement with an interval of 15 seconds brake fade is seen to start at time = 82 s, where the temperature is 565 ºC. It then cools to 545 ºC during the 8 second interval. The next and final engagement brings the maximum temperature to around 652 ºC. The heat is then no longer applied and the brake can cool until t=150 s, the temperature now is 482 ºC. The values for this chart is provided in the appendix.

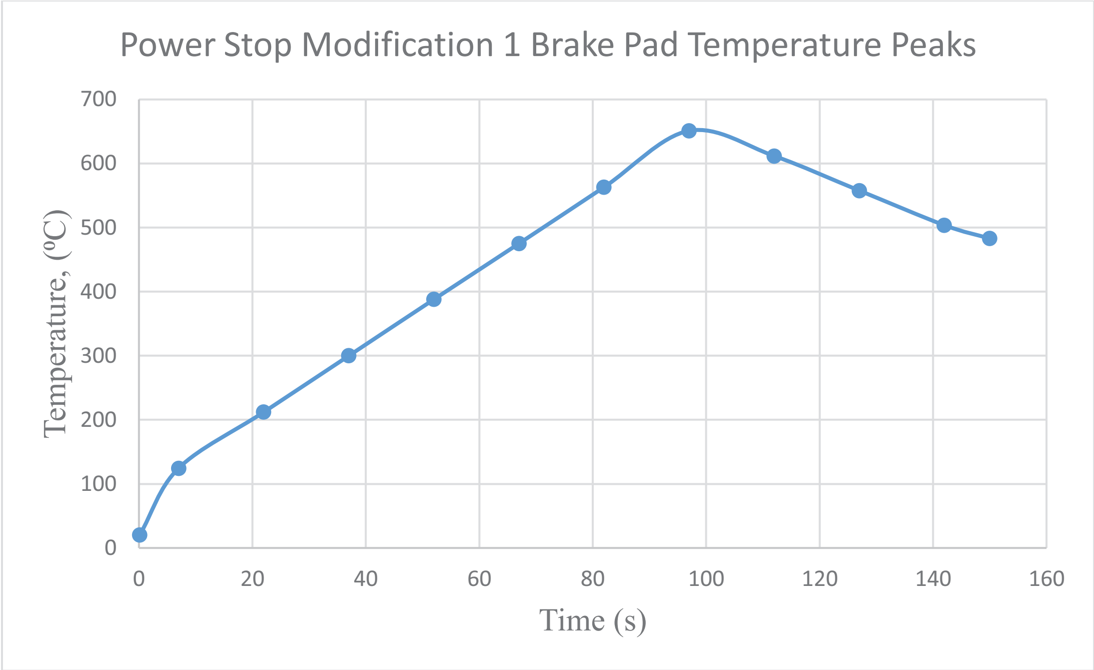

Figure 5.4.4: Temperature peaks for Power Stop Modification 1 brake pad

Figure 5.4.4 shows the maximum temperature of each engagement with respect to time. This is a clear visualization of how the pad increases and decreases in temperature over 150 seconds.

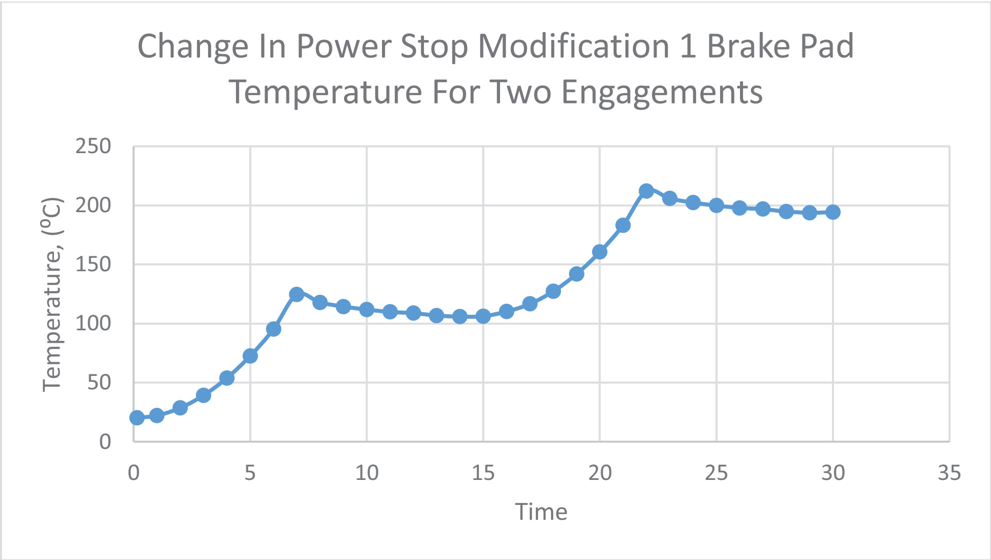

Figure 5.4.5: Power Stop Modification 1 temperature change for 2 engagements

Figure 5.4.5 details the change in temperature with respect to time. An average of a 15 - 20ºC drop can be seen prior to the next brake engagement. This trend is generally followed throughout the simulation.

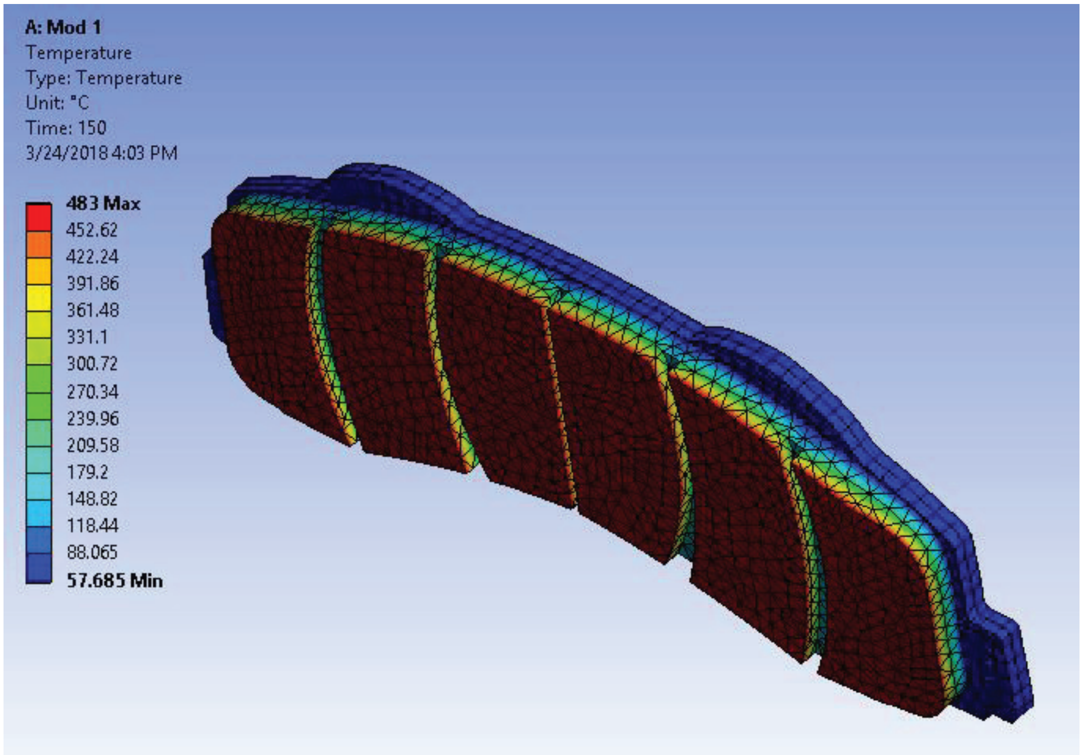

Figure 5.4.6: Modified Power Stop 1 model temperature gradient

5.5 MODIFIED POWER STOP BRAKE PAD WITH TURBULENT AIRFLOW FEATURES

This is the second modified model of the power stop brake pad. The original power stop pad was modified and slots were added to determine if there was any significant impact to the overall cooling of the brake pad.

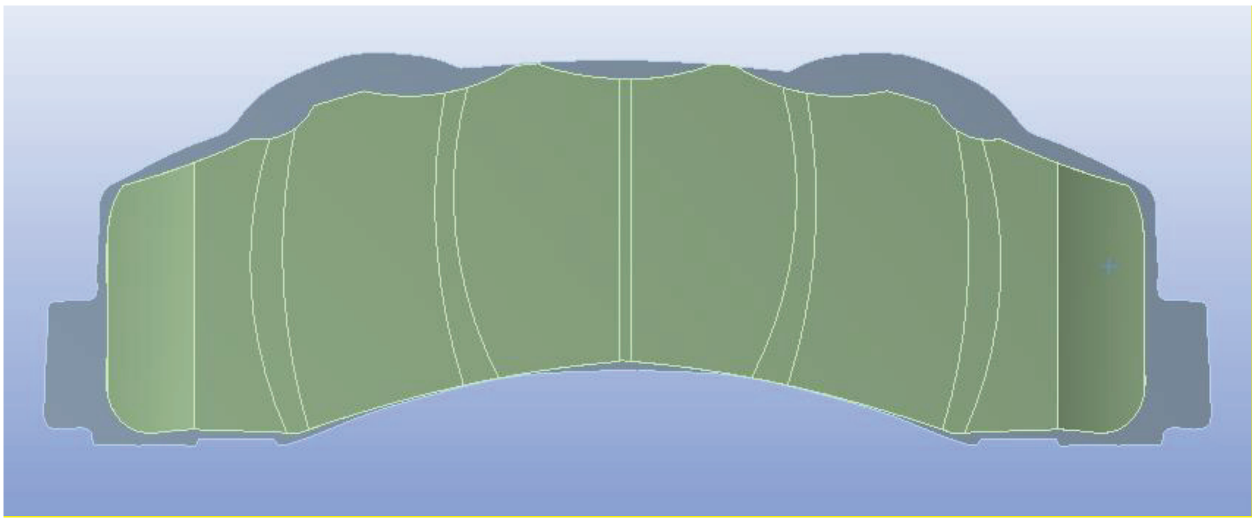

Figure 5.5.1: Modified power stop pad with wavy top designs

For this pad, the curved peaks and valleys generated a turbulence zone that forced air into slots that run from the top to the bottom of the friction material of the pad. This contributed a lot to the overall cooling of the brake pad. The temperatures were significantly cooler brake pad and the final temperature was within a 3% difference of the final Wagner brake pad [26] temperature. Based on this it can be determine that the rounded peaks on the friction material of the pad make a big difference the values that were input for the simulations were initial temperature and convection heat coefficient. The temperatures and heat transfer coefficients are calculated as described in chapter 4.

Table 5.5.1: Modified Power Stop pad 2 convective heat transfer values between 20ºC - 100ºC

				Over all			Slots			Rounded Peaks1			Rounded Peaks2		
Density	Dynamic Viscosity	Conductivity	Prandlt	ReyNolds	Nu	h	ReyNolds	Nu	h	ReyNolds	Nu	h	ReyNolds	Nu	h
1.164	0.00001872	0.02588	0.7282	6.57E+05	484.06	32.967	2.80E+04	99.978	64.686	2.42E+04	92.985	69.55055	3.21E+04	106.9811	60.45133
1.164	0.00001872	0.02588	0.7282	5.56E+05	445.48	30.34	2.37E+04	92.01	59.531	2.05E+04	85.574	64.00769	2.72E+04	98.4552	55.63364
1.164	0.00001872	0.02588	0.7282	4.59E+05	404.79	27.568	1.96E+04	83.605	54.093	1.69E+04	77.757	58.16071	2.24E+04	89.4615	50.55161
1.164	0.00001872	0.02588	0.7282	3.65E+05	360.73	24.568	1.56E+04	74.505	48.205	1.35E+04	69.294	51.83037	1.78E+04	79.72433	45.04947
1.092	0.00001963	0.02735	0.7228	2.43E+05	293.76	21.143	1.04E+04	60.674	41.486	8.97E+03	56.43	44.60591	1.19E+04	64.92408	38.77017
1.092	0.00001963	0.02735	0.7228	1.60E+05	238.66	17.178	6.85E+03	49.294	33.705	5.92E+03	45.846	36.23968	7.84E+03	52.74701	31.49849
1.092	0.00001963	0.02735	0.7228	7.77E+04	166.04	11.95	3.31E+03	34.293	23.448	2.87E+03	31.895	25.2115	3.79E+03	36.69544	21.91311
0.9994	0.00002096	0.02953	0.7154	1.29E+04	67.304	5.2303	5.48E+02	13.901	10.263	4.74E+02	12.929	11.03432	6.28E+02	14.87486	9.590711
0.9994	0.00002096	0.02953	0.7154	12850.2579	67.304	5.2303	5.48E+02	13.901	10.263	4.74E+02	12.929	11.03432	6.28E+02	14.87486	9.590711
0.9994	0.00002096	0.02953	0.7154	8.23E+04	170.28	13.233	3.51E+03	35.17	25.965	3.04E+03	32.71	27.91728	4.02E+03	37.634	24.26489
0.9994	0.00002096	0.02953	0.7154	1.51E+05	230.76	17.932	6.44E+03	47.661	35.186	5.57E+03	44.327	37.83179	7.38E+03	50.9993	32.8823
0.9994	0.00002096	0.02953	0.7154	2.19E+05	277.62	21.574	9.33E+03	57.341	42.332	8.07E+03	53.33	45.51541	1.07E+04	61.35724	39.56068
0.9994	0.00002096	0.02953	0.7154	2.84E+05	316.68	24.609	1.21E+04	65.407	48.287	1.05E+04	60.832	51.91821	1.39E+04	69.98856	45.12581
0.9994	0.00002096	0.02953	0.7154	3.48E+05	350.31	27.223	1.49E+04	72.354	53.416	1.28E+04	67.294	57.43292	1.70E+04	77.42268	49.91903
0.9994	0.00002096	0.02953	0.7154	4.09E+05	379.82	29.516	1.75E+04	78.448	57.914	1.51E+04	72.961	62.26959	2.00E+04	83.94278	54.12293
0.9994	0.00002096	0.02953	0.7154	4.68E+05	405.98	31.549	1.99E+04	83.852	61.904	1.73E+04	77.987	66.55915	2.28E+04	89.72534	57.85129
0.9994	0.00002096	0.02953	0.7154	5.23E+05	429.36	33.366	2.23E+04	88.681	65.469	1.93E+04	82.478	70.39219	2.55E+04	94.89249	61.18286

Table 5.5.2: Modified Power Stop pad 2 Initial FEA inputs, Time = 0s to 15s

time(s)	Temperatures	Convective Over All	Convective Slots	Rounded Peaks	Rounded Peaks 2
0	20	32.96691014	64.68574867	69.55054785	60.45133075
1	26.578	30.33959867	59.53059133	64.00768834	55.63363709
2	33.876	27.5681332	54.09258339	58.16070597	50.55160861
3	45.035	24.56756057	48.20503475	51.83037447	45.04946699
4	60.349	21.1431678	41.48589094	44.60590628	38.77016756
5	81.661	17.17758297	33.70485164	36.23968099	31.49848577
6	105.11	11.95023237	23.44804911	25.21149859	21.91310762
7	132.66	5.230259015	10.26250925	11.0343183	9.590711302
8	[redacted]	5.230259015	10.26250925	11.0343183	9.590711302
9	[redacted]	13.23276952	25.96456871	27.91727723	24.2648924
10	[redacted]	17.93224114	35.18559788	37.83178921	32.88230033
11	[redacted]	21.57427317	42.33178075	45.51541264	39.56068427
12	[redacted]	24.60919518	48.28672774	51.91821132	45.12581225
13	[redacted]	27.22316114	53.41569933	57.43291573	49.91903432
14	[redacted]	29.51574227	57.91406832	62.26959203	54.1229339
15	[redacted]	31.54898892	61.90358634	66.55914838	57.85129259

Table 5.5.1 show the respective density, dynamic viscosity, thermal conductivity, Prandtl's number, calculations for the Reynolds number, Nusselt's number and finally the convective heat transfer coefficient for the modified power stop 2 pad. These values change over time as well as temperature, further tables are included in the appendix.

Table 5.5.2 is the values that are input into ANSYS [24], at time = 8 s the heating is stopped while the convective heat transfer coefficient remains in effect until time = 15 (s). At t = 15(s) the brakes are then engaged again, and the heat is the applied to for 7 seconds (100 km/h to 5km/h) and the cycle then continues.

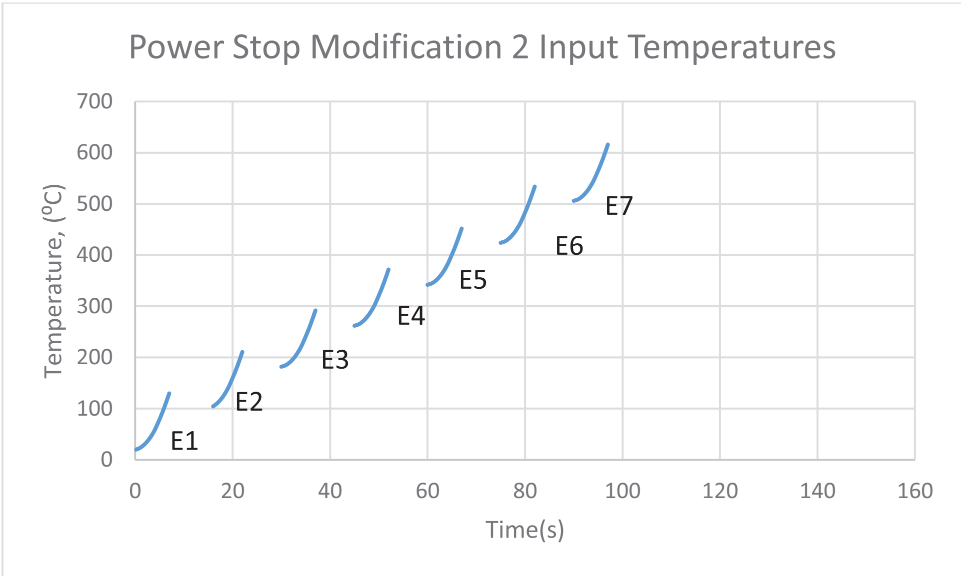

Figure 5.5.2: Summary of Power Stop modification 2 temperature inputs

The finite element analysis temperatures that were input into ANSYS [24] for the modified power stop 2 brake pads is summarized in Figure 5.5.2. The values are provided in the appendix. Heat is initially applied for 7 seconds, allowed to cool for 8 seconds (for the vehicle to get up to speed) and then applied again. This is repeated until brake fade temperatures of above 550 ºC are reached.

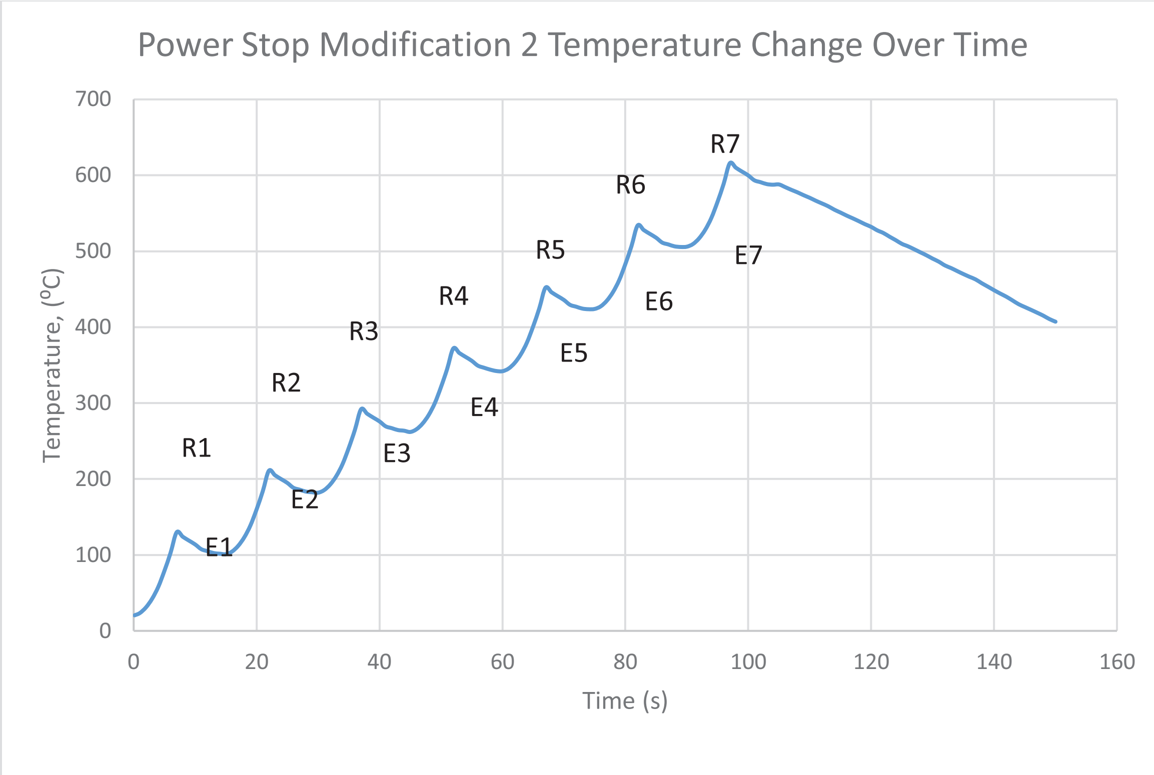

Figure 5.5.3 Temperature change for Power Stop Modification 2 brake pad over Time

The ambient temperature is 20ºC and on average each engagement raises the average temperature by 112.8 ºC. This increase is even larger than the original power stop brake pad and the modified power stop 1 brake pad. Once again in addition to the slots that are cut into the pad material was removed at the top to create air turbulence zone. The mass of the now is lesser than and based on the caloric heat equation, the change in temperature becomes larger. While the vehicle is then brought up to speed the pad loses an average of about 25-30 ºC in 8 seconds. After 7 repeated engagements, each engagement with an interval of 15 seconds brake fade is seen to start at time = 82 s, where the temperature is 536.79 ºC. It then cools to 505 ºC during the 8 second interval. The next and final engagement brings the maximum temperature to around 618ºC. The heat is then no longer applied and the brake cools until t=150 s, the temperature now is 407.22 ºC. This shows that the addition of convective peaks, valleys and slots helps decrease the temperature of the pads drastically. There was a 16% difference in the final temperature between the original PowerStop pad and the 2nd modified pad. The values for this chart is provided in the appendix.

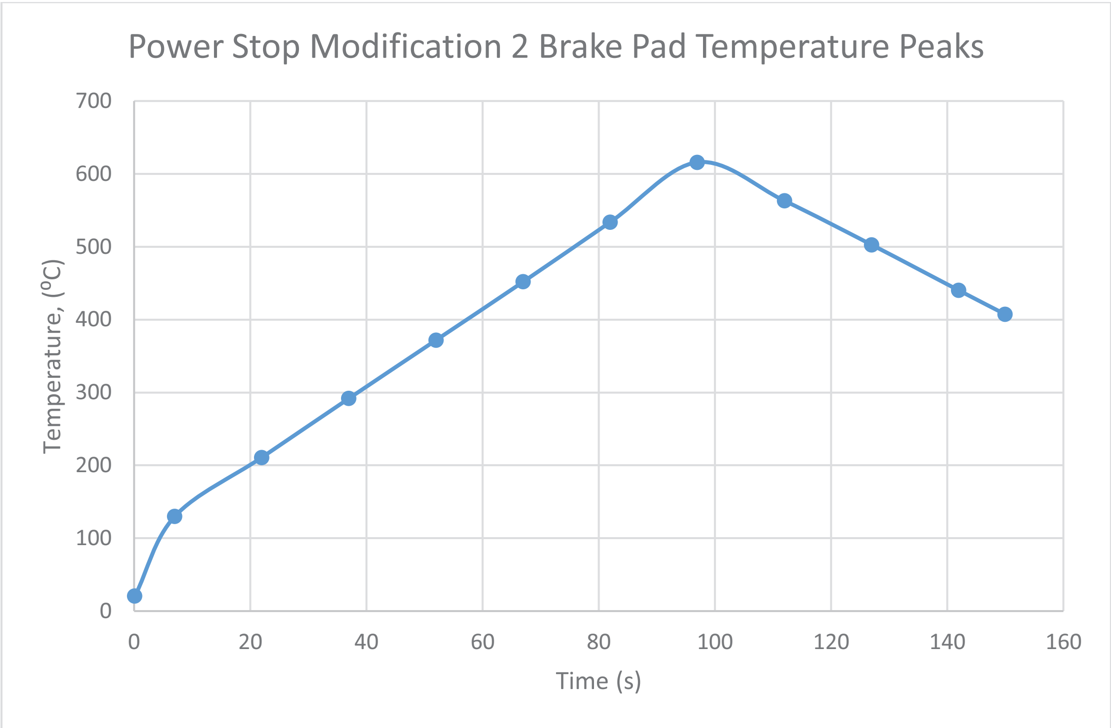

Figure 5.5.4: Temperature peaks for Power Stop Modification 2 brake pad

Figure 5.5.4 shows the maximum temperature of each engagement with respect to time. This is a clear visualization of how the pad increases and decreases in temperature over 150 seconds.

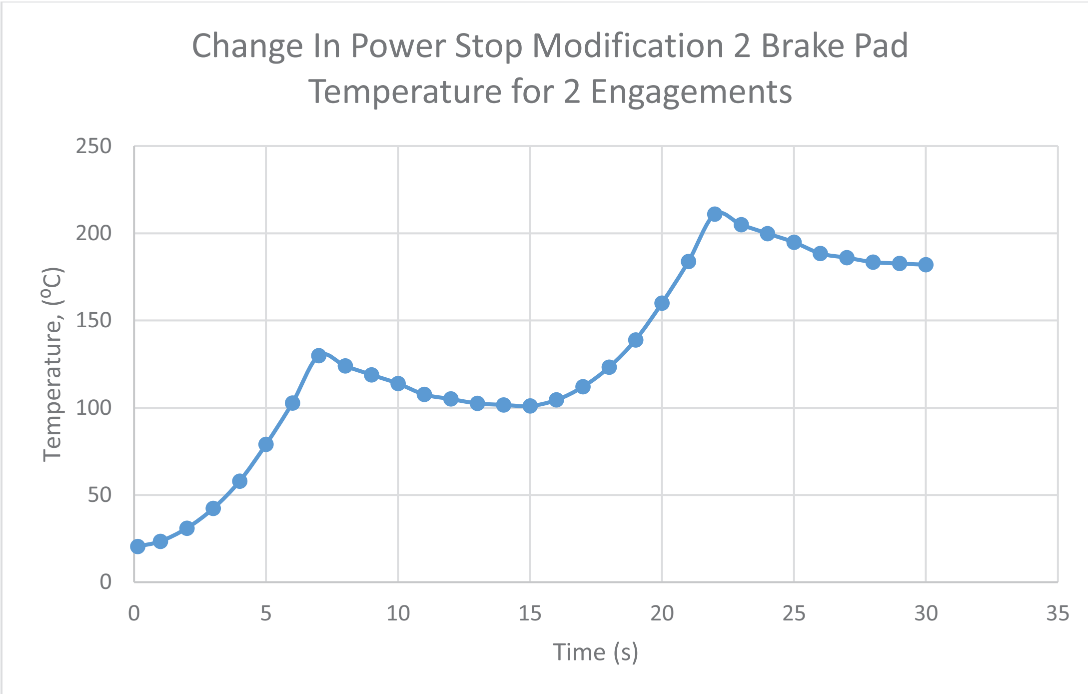

Figure 5.5.5: Power Stop Modification 2 Temperature change for 2 engagements

Figure 5.5.5 details the change in temperature with respect to time. An average of a 25 – 30ºC drop can be seen prior to the next brake engagement. This trend is generally followed throughout the simulation.

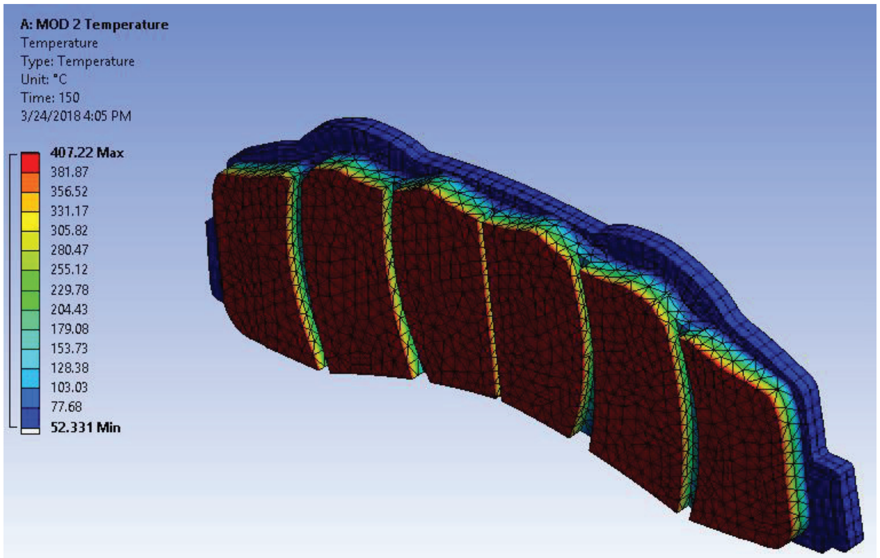

Figure 5.5.6: Modified Power Stop 2 Model temperature gradient

CHAPTER 6 – FUTURE WORK

6.1 FUTURE WORK

For the future, brake pads with different geometries should be studied. A model with inlets and outlets on the side such as the one included in the appendix should be analyzed.

Tools have been created in this research to help in future work. Spreadsheets to calculate, temperature increase due to vehicle weight, drag area, velocity, coefficient of rolling resistance and coefficient of drag have been developed. Spreadsheets to calculate convective heat transfer coefficients also have been developed, the inputs merely required are the characteristic length, of the object being studied. The specified methodology for this research should be improved to consider side airflow and the test need not be limited to intervals of 100km/h to 5 km/h. The mesh size of the brake pads should also be increased to attain more accurate values

6.2 DISCUSSION

Comparison to on the road test

This research only considered the effects of air generated by the wheel for cooling of the brake pad. For an on the road test, air due to the vehicle moving in the direction respective to the fluid will also play a role in cooling the brake pads faster. Based on this, there is a chance the brake pad temperatures will be cooler than determined from this study.

Ventilated Rotor Design

A ventilated rotor design, may cause disruptions in the flow of air and temperature of air around the brake pads. Based on this, the brake pads may not cool as expected due to either the lack of cool air or the disruption of flow to where the turbulence zones do not force air into the slots to promote greater convective cooling

Initial Methodology Considered

During the initial stages of this study, the heating in the brake pad due to coefficient of friction was considered. The following method was considered. This was however abandoned because the coefficient of drag and rolling resistance could not be calculated accurately especially due to changing velocities and airflow.

The method is included below for future reference:

Based on AK master test parameters, the vehicle is travelling with an initial velocity of 100 km/h (27.7 m/s) and it needs to be decelerated by 0.4 times gravitational acceleration to 5 km/h (1.38 m/s). Using equations (1) and (2), the time (s) for this brake engagement as well as the distance required to slow down to 1.38 m/s can be found.

$$\frac{(Vf - Vi)}{a} = t \quad (16)$$

To find the stopping distance:

$$\mathrm{d} = \frac{Vi + Vf}{2} * t \qquad (17)$$

This distance is the distance travelled by the wheel. This information can then be used to find the sliding distance of the brake pad and rotor assembly by using the ratios of the wheel assembly radius and rotor radius. Based on the Goodyear website, the radius of a regular Ford F-150 single cab tire is 0.4073 m and based on the AutoZone website, an average brake rotor for the same vehicle is 0.175 m:

$$\frac{r_r}{r_w} = \frac{d_r}{d_w} \text{ which can be simplified to } d_r = \frac{r_r}{r_w} * d_w \qquad (18)$$

The measurement of the brake pads was done by hand, and the total contact area was determined to be 0.0072 m^2. This, however, is subject to change for future analysis as the geometry will be optimized for greater heat dissipation. This could mean either an increase or decrease in contact area. Once again, AK master test parameters are used, and the pressure is going to be set at 30 Bar (300000 Pa). The normal load can be calculated using equation 4:

$$Fn = P * A \qquad (19)$$

This normal load can then be multiplied with the coefficient of friction to determine the friction force. The equation that will be used is:

$$Ff = Fn * \mu f \qquad (20)$$

AK Master test parameters specify coefficient of friction ranges between 0.1 to 0.6. For this calculation, we will use a value of 0.5 as it is the average value for the brake engagements in the AK Master tests. The total energy can then be calculated using the following formula:

$$E = Ff * dr \qquad (21)$$

Out of the total energy, it is assumed that only 95% is converted into thermal energy. The other 5% is dissipated by other means.

$$Q = 0.95\,E \qquad (22)$$

Finally, the change in temperature can be calculated using the following equation:

$$Q = m\,c\,\Delta t \qquad (23)$$

From literature review the average specific heat value for brake pads are 900 J kg^{-1} K^{-1} and the mass of an average brake pad for the ford F-150 is 0.70 kg.

FEA VALIDATION TEST INSTRUCTIONS

This test was not part of the original goals of the thesis, however it was important to develop method to validate the FEA results. This can be seen in chapter 4.4. Due to the nature of the study, it was decided that the pads would be burnished using the International Organization for Standardization test. Information on this test can be seen in Chapter 4.4 of this thesis. The following were methods suggested by the manufacturer, these methods were not used to burnish the pads, instead the ISO standard was used.

Wagner Burnishing (Wagner Website)

- Make approximately 20 “Complete Stops” from 30-mph or 20 “Slow-Downs” from 50-mph to 20-mph with light to moderate pedal pressure
- No Panic Stops
- Allow at least 30 seconds between brake applications for the brake pads or shoes to cool down
- It is critical to follow cool down procedures to avoid damaging NAO, Ceramic and Semi-Met friction material as well as the rotor/drum
- No high-speed stops and/or braking under heavy loads that could result in glazed or otherwise damaged linings

Power Stop Burnishing (PowerStop Website)

- 5 moderates to aggressive stops from 40 mph down to 10 mph in rapid succession without letting the brakes cool and do not come to a complete stop. If you're forced to stop, either shift into neutral or give room in front so you can allow the vehicle to roll slightly while waiting for the light. The rotors will be very hot and holding down the brake pedal will allow the pad to create an imprint on the rotor. This is where the judder can originate from.

- Then do 5 moderate stops from 35 mph to 5 mph in rapid succession without letting the brakes cool. You should expect to smell some resin as the brakes get hot.
- After this is complete, drive around for as long as possible without excessively heating the brakes and without coming to a complete stop (Try for about 5 minutes at moderate speed). This is the cooling stage. It allows the heated resin in the brake pads to cool and cure.
- After the brakes have cooled to standard operating temperature, you may use the brakes normally.

REFERENCES

1) Koç, O. 2008. Results of the friction brake pad including heat transfer system and thermal analysis, Master of Science Thesis, Afyon Kocatepe University, Institute of Science, (In Turkey).
2) Domaç, G.S. 2006. Disc brakes of the design and tribological examination, PhD Thesis, Yildiz Technical University, Institute of Science, (In Turkey).
3) Timur, M., & Kuşçu, H. (2014). Heat transfer of brake pad used in the autos after friction and examination of thermal tension analysis. Mechanics,20(1).
4) Belhocine, A., and M. Bouchetara. "Simulation of Fully Coupled Thermomechanical Analysis of Automotive Brake Discs". SIMULATION 88.8 (2011): 921-935. Web.
5) Talati, Faramarz, and Salman Jalalifar. "Analysis of Heat Conduction in A Disk Brake System". Heat and Mass Transfer 45.8 (2009): 1047-1059. Web.
6) Grigoratos, T. & Martini, G. Environ Sci Pollut Res (2015) 22: 2491.
7) Belhocine, A. et al. "Modeling of Thermal Contact Problem of Disc Brake System with Frictional Heat Generation". World Journal of Engineering 11.4 (2014): 373-390. Web.
8) Gao CH, Lin XZ (2002) Transient temperature field analysis of a brake in a non-axisymmetric three-dimensional model. J Mat Proc Tech 129:513–517. doi:10.1016/S0924-0136(02)00622-2
9) Voldrˇich J (2006) Frictionally excited thermoelastic instability in disc brakes—Transient problem in the full contact regime. Int J Mech Sci 49(2):129–137.

V. Chengal Reddy, M. Gunasekhar Reddy, “Modeling and Analysis of FSAE Car Disc Brake Using FEM” International Journal of Emerging Technology and Advanced Engineering, Vol.3, PP 383-389, 2013.

10) TV. Manjunath, and P.M. Suresh. Structural and Thermal Analysis of Rotor Disc of Disc Brake, International Journal of Innovative Research in Science, Vol. 2, Issue 12, (2013) pp.7741-7749
11) Liu. Cheng, E. et al “Effect of chamfered brake pad patterns on the vibration squeal response of disc brake system”. 3rd International Symposium on Advanced Fluid/Solid Science and Technology in Experimental Mechanics, 7-10 December. 2008, Taiwan.
12) "What Is Brake Fade?" EBC Brakes. N.p., n.d. Web. 24 Apr. 2017.
13) Hunter, J. E., S. S.Cartier, et al. (1998). Brake Fluid Vaporization as a Contributing Factor in Motor Vehicle Collisions. International Congress and Exposition, Detroit, Michigan, SAE
14) Stephens, A et al. (2006). Aerodynamic cooling of automotive disc brakes, Department of Mechanical engineering RMIT University, Melbourne
15) Little, E., T.-K. Kao, et al. (1998). “A Dynamometer Investigation of Thermal Judder.” 81-89.
16) Noyes, R. N. and P. T. Vickers (1969). Prediction of Surface Temperatures in Passenger Car Disc Brakes.
17) Çengel, Yunus A., et al. Heat and Mass Transfer: Fundamentals & Applications. McGraw Hill Education (New York), 2016.
18) Blau, Peter J. Friction science and technology: from concepts to applications. CRC press,2008.

19) Krusemann, R. and G. Schmidt (1995). Analysis and optimization of Disk Brake Cooling via Computational Fluid Dynamics. International Congress and Exposition, Detroit, Michigan, SAE.

20) Walker, J., Resnick, R., & Halliday, D. (2014). Halliday & Resnick fundamentals of physics. Hoboken, NJ: Wiley.

21) "OEx Brake Pads," Wagner Brake | Brake Pads, Brake Rotors & Headlights. [Online]. Available: http://www.wagnerbrake.com/products/brakes/wagner-oex.html. [Accessed: 03-Apr-2018].

22) "Performance Brake Upgrade Kits for Sport, Utility and Daily Driving | Power Stop Brakes," Power Stop. [Online]. Available: https://www.powerstop.com/. [Accessed: 03-Apr-2018].

23) "Dynamometer Global Brake Effectiveness J2522_200306," J2522: Dynamometer Global Brake Effectiveness - SAE International. [Online]. Available: https://doi.org/10.4271/J2522_200306. [Accessed: 03-Apr-2018].

24) ANSYS® Academic Research Mechanical, Release 18.2 Thermal Transient Analysis, ANSYS, Inc.

25) ANSYS® Space Claim, Release 18.2, ANSYS, Inc.

26) C. R. Buxton, R. G. Silvey, and W. Liu, "Vehicle brake friction pad." U.S. Patent No. USD787393S1 (01 September 2015)

APPENDICES

APPENDIX A – BRAKE HEATING OVER TIME

Table 7.1.1: Input data for brake pad heat calculations

Deceleration			-0.4	G
Acceleration			0.4	G
Mass			2045.45455	kg
Tire Pressure			2.5	Bar
Gravity			9.81	m/s
Drag Coeff			0.4	-
Density of air			1.225	kg/m^3
Area Exposed			2.94	m^2
Initial V			27.8	
Weight (LB)			4500	
Weight (kg)				
Tamb			20	Celsius
Brake Ratio		Front %	Rear %	
		70	30	
BP Area		0.197	0.101	0.019897

Table 7.1.2: Values of rolling resistance coefficient, rolling resistance force (N), drag force (N), sum of forces (N) and acceleration through sum of forces method m/s^2 over time

Time (s)	Time (m)	Rolling resistance coefficient	Rolling resistance force (N)	Drag Force (N)	Sum of forces (N)	Acceleration through sum of forces method m/s^2
0	0	0.01280608	256.965686	556.676652	813.6423379	-0.397780699
0.25	0.004166667	0.01251599	251.144621	514.2471	765.3917202	-0.374191508
0.5	0.008333333	0.01224037	245.614055	473.93499	719.5490455	-0.351779533
0.75	0.0125	0.01197864	240.362224	435.65457	676.0167944	-0.330497099
1	0.016666667	0.01173026	235.378398	399.327626	634.7060242	-0.310300723
1.25	0.020833333	0.01149476	230.65279	364.882828	595.5356188	-0.291150747
1.5	0.025	0.01127168	226.17648	332.255153	558.4316336	-0.273011021
1.75	0.029166667	0.01106062	221.941343	301.385379	523.3267219	-0.25584862
2	0.033333333	0.01086121	217.93999	272.219645	490.1596347	-0.239633599
2.25	0.0375	0.01067311	214.165713	244.709068	458.8747813	-0.224338782
2.5	0.041666667	0.01049603	210.612443	218.809403	429.4218467	-0.209939569
2.75	0.045833333	0.01032969	207.274707	194.48075	401.7554571	-0.196413779
3	0.05	0.01017385	204.14759	171.6873	375.8348902	-0.183741502
3.25	0.054166667	0.01002829	201.226711	150.397113	351.6238238	-0.171904981
3.5	0.058333333	0.00989281	198.508194	130.581928	329.0901212	-0.160888504
3.75	0.0625	0.00976724	195.988643	112.217006	308.2056484	-0.150678317
4	0.066666667	0.00965145	193.665129	95.2809934	288.9461228	-0.141262549
4.25	0.070833333	0.0095453	191.535174	79.7558152	271.2909888	-0.13263115
4.5	0.075	0.0094487	189.596733	65.6265878	255.223321	-0.124775846
4.75	0.079166667	0.00936156	187.848196	52.8815573	240.7297532	-0.117690102
5	0.083333333	0.00928382	186.288373	41.5120585	227.8004314	-0.1113691
5.25	0.0875	0.00921546	184.916496	31.5124956	216.4289919	-0.105809729
5.5	0.091666667	0.00915644	183.73222	22.8803439	206.6125637	-0.101010587
5.75	0.095833333	0.00910677	182.735622	15.616174	198.3517958	-0.096971989
6	0.1	0.00906648	181.927211	9.72369776	191.6509092	-0.093696
6.25	0.104166667	0.00903562	181.307939	5.20983796	186.5177765	-0.091186469
6.5	0.108333333	0.00901425	180.879206	2.08482242	182.9640286	-0.089449081
6.75	0.1125	0.00900248	180.642888	0.36230454	181.0051922	-0.088491427
7	0.116666667	0.00900041	180.601347	0.05951245	180.660859	-0.088323087
7	0.116666667	0.00900041	180.601347	0.05951245	180.660859	-0.088323087

Table 7.1.3: Values of total acceleration m/s², acceleration %. speed m/s, speed km/h, distance (m), energy (J) over time

Total Acceleration m/s^2	Acceleration %	Speed m/s	Speed km/h	Distance (m)	Energy (J)
-4.3217807	0.092040926	27.8	100.08	0	0
-4.2981915	0.087057896	26.7195548	96.1903974	6.814944353	1193.89272
-4.2757795	0.082272608	25.6509042	92.3432553	13.36272606	4723.58103
-4.2544971	0.077681825	24.5931653	88.5353953	19.64743701	10517.5109
-4.2343007	0.073282637	23.5455029	84.7638104	25.67275145	18512.1262
-4.2151507	0.06907244	22.5071241	81.0256467	31.44195256	28651.2293
-4.197011	0.065048917	21.4772739	77.318186	36.95795541	40885.4307
-4.1798486	0.06121002	20.4552307	73.6388306	42.22332687	55171.6731
-4.1636336	0.057553959	19.4403028	69.9850899	47.24030276	71472.8229
-4.1483388	0.054079185	18.4318244	66.3545678	52.01080245	89757.3212
-4.1339396	0.050784383	17.429153	62.744951	56.53644131	109998.886
-4.1204138	0.04766846	16.4316662	59.1539983	60.818541	132176.264
-4.1077415	0.044730542	15.4387587	55.5795312	64.85813799	156273.021
-4.095905	0.041969963	14.4498401	52.0194244	68.65599019	182277.377
-4.0848885	0.039386266	13.4643326	48.4715972	72.21258199	210182.073
-4.0746783	0.036979193	12.4816681	44.9340052	75.52812771	239984.276
-4.0652625	0.03474869	11.5012867	41.4046322	78.60257346	271685.51
-4.0566312	0.0326949	10.5226342	37.881483	81.4355976	305291.629
-4.0487758	0.030818166	9.54515982	34.3625754	84.02660961	340812.808
-4.0416901	0.029119032	8.56831473	30.845933	86.37474749	378263.575
-4.0353691	0.027598244	7.59154949	27.3295782	88.47887373	417662.869
-4.0298097	0.026256756	6.61431223	23.811524	90.33756959	459034.125
-4.0250106	0.025095732	5.63604649	20.2897674	91.94912784	502405.4
-4.020972	0.024116554	4.65618913	16.7622809	93.31154374	547809.527
-4.017696	0.023320829	3.67416807	13.227005	94.4225042	595284.307
-4.0151865	0.022710394	2.6894	9.68184	95.279375	644872.738
-4.0134491	0.022287334	1.70128795	6.12463664	95.87918585	696623.288
-4.0124914	0.022053985	0.70921871	2.55318734	96.21861313	750590.214
-4.0123231	0.022012955	-0.28744	-1.034784	96.29396003	806833.928
-4.0123231	0.022012955	-0.28744	-1.034784	96.29396003	

Table 7.1.4: Values of brake energy, front energy, rear energy, left energy, inner pad energy and rotor delta T over time

Energy Brakes(J)	Δ Front Energy	Δ Rear Energy	Left Energy	Inner	Rotor del t
0	0	0	0	0	0
1089.95494	762.968456	326.986481	381.4842	190.742114	0.07143899
4334.9597	3034.47179	1300.48791	1517.236	758.617947	0.28412657
9700.49149	6790.34405	2910.14745	3395.172	1697.58601	0.6358
17155.5087	12008.8561	5146.65262	6004.428	3002.21403	1.12442473
26672.219	18670.5533	8001.6657	9335.277	4667.63832	1.74817915
38225.8777	26758.1144	11467.7633	13379.06	6689.5286	2.50544142
51794.6138	36256.2297	15538.3841	18128.11	9064.05742	3.39477806
67359.2789	47151.4953	20207.7837	23575.75	11787.8738	4.41493401
84903.3184	59432.3229	25470.9955	29716.16	14858.0807	5.56482424
104412.661	73088.8625	31323.7982	36544.43	18272.2156	6.84352645
125875.625	88112.9376	37762.6875	44056.47	22028.2344	8.25027505
149282.844	104497.991	44784.8533	52249	26124.4978	9.78445609
174627.202	122239.042	52388.1607	61119.52	30559.7604	11.4456032
201903.786	141332.651	60571.1359	70666.33	35333.1626	13.2333942
231109.851	161776.896	69332.9553	80888.45	40444.2239	15.1476494
262244.794	183571.356	78673.4383	91785.68	45892.839	17.1883292
295310.149	206717.104	88593.0448	103358.6	51679.2761	19.3555341
330309.582	231216.707	99092.8746	115608.4	57804.1769	21.6495044
367248.906	257074.235	110174.672	128537.1	64268.5586	24.0706212
406136.107	284295.275	121840.832	142147.6	71073.8188	26.6194078
446981.378	312886.965	134094.413	156443.5	78221.7411	29.2965323
489797.168	342858.018	146939.151	171429	85714.5045	32.1028107
534598.249	374218.774	160379.475	187109.4	93554.6935	35.0392111
581401.783	406981.248	174420.535	203490.6	101745.312	38.1068585
630227.423	441159.196	189068.227	220579.6	110289.799	41.3070409
681097.412	476768.188	204329.224	238384.1	119192.047	44.6412161
734036.708	513825.696	220211.012	256912.8	128456.424	48.1110202
789073.129	552351.191	236721.939	276175.6	138087.798	51.7182763

Table 7.1.5: Values for temperature of brake pad delta T, inner temperature and final temperature increase over time.

BP del t	Inner	Temp
0	0	20
0.31167012	0.15583506	20.15583506
1.23957181	0.6197859	20.6197859
2.77383335	1.38691668	21.38691668
4.90557848	2.45278924	22.45278924
7.62686001	3.81343	23.81343
10.9306023	5.46530115	25.46530115
14.8105513	7.40527567	27.40527567
19.2612317	9.63061586	29.63061586
24.2779097	12.1389548	32.13895483
29.8565615	14.9282807	34.92828074
35.9938471	17.9969235	37.99692353
42.6870878	21.3435439	41.34354392
49.9342491	24.9671245	44.96712453
57.7339259	28.8669629	48.86696294
66.0853332	33.0426666	53.04266658
74.988299	37.4941495	57.49414952
84.4432616	42.2216308	62.22163082
94.4512694	47.2256347	67.2256347
105.013985	52.5069923	72.50699235
116.133691	58.0668454	78.06684542
127.813303	63.9066513	83.90665126
140.05638	70.0281899	90.02818994
152.867146	76.4335731	96.43357313
166.25051	83.125255	103.125255
180.21209	90.106045	110.106045
194.758247	97.3791234	117.3791234
209.896118	104.948059	124.9480588
225.633656	112.816828	132.8168281

APPENDIX B – CONVECTIVE HEAT TRANSFER VALUES

Table 7.2.1: Linear velocity, revolutions per second, radians per second, tangential velocity, slot tangential velocity, temperatures and film temperature values for convection heat transfer coefficient.

		Linear V	RPS	rad/s	V tan	V tan (Slots)	Temp	T film
0	0	27.8	11.6419	73.1579	27.8	11.2663158	30	30
1	1	23.5455	9.86026	61.9618	23.5455	9.54212486	32.2239	31.1119
2	2	19.4403	8.1411	51.1587	19.4403	7.87843849	38.7318	34.3659
3	3	15.4388	6.46536	40.6283	15.4388	6.25676009	49.3515	39.6757
4	4	11.5013	4.81645	30.2665	11.5013	4.66104778	63.9947	46.9973
5	5	7.59155	3.17915	19.9778	7.59155	3.07657532	82.6473	56.3236
6	6	3.67417	1.53865	9.66886	3.67417	1.48900495	105.367	67.6834
7	7	0.70922	0.297	1.86637	0.70922	0.28742021	132.287	81.1436
8	0	0.70922	0.297	1.86637	0.70922	0.28742021	132.287	81.1436
9	1	4.53978	1.90115	11.9468	4.53978	1.8398076	132.287	81.1436
10	2	8.33687	3.49127	21.9391	8.33687	3.37862548	132.287	81.1436
11	3	12.0672	5.05343	31.7558	12.0672	4.89038735	132.287	81.1436
12	4	15.701	6.5752	41.3185	15.701	6.36305583	132.287	81.1436
13	5	19.2137	8.04621	50.5624	19.2137	7.78660277	132.287	81.1436
14	6	22.5861	9.45848	59.4371	22.5861	9.15331337	132.287	81.1436
15	7	25.805	10.8065	67.908	25.805	10.4578354	132.287	81.1436
16	8	28.8628	12.087	75.9547	28.8628	11.6970214	132.287	81.1436

Table 7.2.2: Density, Dynamic viscosity, thermal conductivity, Prandtl, Reynold, Nusselt's values for convection heat transfer coefficient.

Temp Taken	Density	Dynamic Viscosity	Conductivity	Prandtl	Reynolds	Nu	h
30	1.164	0.00001872	0.02588	0.7282	6.57E+05	484.058	32.9669
30	1.164	0.00001872	0.02588	0.7282	5.56E+05	445.481	30.3396
30	1.164	0.00001872	0.02588	0.7282	4.59E+05	404.787	27.5681
30	1.164	0.00001872	0.02588	0.7282	3.65E+05	360.729	24.5676
50	1.092	0.00001963	0.02735	0.7228	2.43E+05	293.762	21.1432
50	1.092	0.00001963	0.02735	0.7228	1.60E+05	238.665	17.1776
50	1.092	0.00001963	0.02735	0.7228	7.77E+04	166.036	11.9502
80	0.9994	0.00002096	0.02953	0.7154	1.29E+04	67.3044	5.23026
80	0.9994	0.00002096	0.02953	0.7154	1.28E+04	67.3044	5.23026
80	0.9994	0.00002096	0.02953	0.7154	8.23E+04	170.283	13.2328
80	0.9994	0.00002096	0.02953	0.7154	1.51E+05	230.757	17.9322
80	0.9994	0.00002096	0.02953	0.7154	2.19E+05	277.624	21.5743
80	0.9994	0.00002096	0.02953	0.7154	2.84E+05	316.678	24.6092
80	0.9994	0.00002096	0.02953	0.7154	3.48E+05	350.315	27.2232
80	0.9994	0.00002096	0.02953	0.7154	4.09E+05	379.817	29.5157
80	0.9994	0.00002096	0.02953	0.7154	4.68E+05	405.981	31.549
80	0.9994	0.00002096	0.02953	0.7154	5.23E+05	429.361	33.3658

Table 7.2.3: Slot Reynolds and Nusselt's *values for convection heat transfer coefficient.*

ReyNolds	Nu	h	ReyNolds	Nu	h
2.80E+04	99.978	64.6857	2.10E+04	86.5835	74.692669
2.37E+04	92.0102	59.5306	1.78E+04	79.6832	68.740006
1.96E+04	83.6052	54.0926	1.47E+04	72.4043	62.460735
1.56E+04	74.5055	48.205	1.17E+04	64.5236	55.66238
1.04E+04	60.6741	41.4859	7.78E+03	52.5453	47.903781
6.85E+03	49.2941	33.7049	5.13E+03	42.69	38.91901
3.31E+03	34.2933	23.448	2.48E+03	29.6989	27.075475
5.48E+02	13.9011	10.2625	4.11E+02	12.0387	11.850125
548.1827483	13.9011	10.2625	411.1371	12.0387	11.850125
3.51E+03	35.1704	25.9646	2.63E+03	30.4585	29.981301
6.44E+03	47.6608	35.1856	4.83E+03	41.2755	40.628829
9.33E+03	57.3407	42.3318	7.00E+03	49.6585	48.88053
1.21E+04	65.407	48.2867	9.10E+03	56.6441	55.756711
1.49E+04	72.3545	53.4157	1.11E+04	62.6608	61.679137
1.75E+04	78.4478	57.9141	1.31E+04	67.9378	66.873406
1.99E+04	83.8518	61.9036	1.50E+04	72.6178	71.480104
2.23E+04	88.6807	65.4685	1.67E+04	76.7997	75.59654

APPENDIX C – FINAL BRAKE PAD TEMPERATURES OVER TIME

Table 7.3.1: Final Temperatures for 4 brake pad models

Time(s)	PowerStop	Wagner	Mod 1	Mod 2
0.14	20.538	20.311	20.683	20.845
1	23.844	22.224	22.694	23.458
2	30.352	28.732	29.202	30.966
3	40.971	39.351	39.821	42.285
4	55.615	53.995	54.465	57.929
5	74.267	72.647	73.117	79.011
6	96.987	95.367	95.837	102.76
7	123.91	122.29	125.1	129.93
8	119.59	116.54	117.84	123.93
9	116.12	111.56	114.37	118.86
10	113.58	107.06	111.83	113.89
11	111.57	103.06	109.82	107.58
12	110.56	101.19	108.81	104.99
13	108.54	100.12	106.79	102.49
14	107.53	99.267	104.78	101.64
15	108	100	105.25	101
16	111.84	102.22	109.09	104.46
17	118.35	108.73	115.6	111.97
18	128.97	119.35	126.22	123.29
19	143.62	133.99	140.87	138.93
20	162.27	152.65	159.52	160.01
21	184.99	175.37	182.24	183.76
22	211.91	202.29	211	210.93
23	207.59	196.54	204.84	204.93
24	204.12	191.56	201.37	199.86
25	201.58	187.06	198.83	194.89
26	199.57	183.06	196.82	188.44
27	198.56	181.19	195.81	185.99
28	196.54	180.12	193.79	183.49
29	195.53	179.27	192.78	182.64
30	196	178	193.25	182
31	199.84	180.22	197.09	185.46
32	206.35	186.73	203.6	192.97
33	216.97	197.35	214.22	204.29
34	231.62	211.99	228.87	219.93
35	250.27	230.65	247.52	241.01

36	272.99	253.37	270.24	264.76
37	299.91	280.29	299	291.93
38	295.59	274.54	292.84	285.93
39	292.12	269.56	289.37	280.86
40	289.58	265.06	286.83	275.89
41	287.57	261.06	284.82	269.44
42	286.56	259.19	283.81	266.99
43	284.54	258.12	281.79	264.49
44	283.53	257.27	280.78	263.64
45	284	258	281.25	262
46	287.84	260.22	285.09	265.46
47	294.35	266.73	291.6	272.97
48	304.97	277.35	302.22	284.29
49	319.61	291.99	316.86	299.93
50	338.27	310.65	335.52	321.01
51	360.99	333.37	358.24	344.76
52	387.91	360.29	387	371.93
53	383.59	354.54	380.84	365.93
54	380.12	349.56	377.37	360.86
55	377.58	345.06	374.83	355.81
56	375.57	341.06	372.82	349.36
57	374.56	339.19	371.81	346.61
58	372.54	338.12	369.79	344.11
59	371.53	337.27	368.78	342.26
60	373	338	370.25	342
61	376.84	340.22	374.09	345.46
62	383.35	346.73	380.6	352.97
63	393.97	357.35	391.22	364.29
64	408.61	371.99	405.86	379.93
65	427.27	390.65	424.52	401.01
66	449.99	413.37	447.24	424.76
67	476.91	440.29	474.16	451.93
68	472.59	434.54	469.84	445.93
69	469.12	429.56	466.37	440.86
70	466.58	425.06	463.83	435.89
71	464.57	421.06	461.82	429.44
72	463.56	419.19	460.81	426.99
73	461.54	418.12	458.79	424.49
74	460.53	417.27	457.78	423.64
75	461	418	458.25	424
76	464.84	420.22	462.09	427.46

77	471.35	426.73	468.6	434.97
78	481.97	437.35	479.22	446.29
79	496.61	451.99	493.86	461.93
80	515.27	470.65	512.52	483.01
81	537.99	493.37	535.24	506.76
82	564.91	520.29	562.16	533.93
83	560.59	514.54	557.84	527.93
84	557.12	509.56	554.37	522.86
85	554.58	505.06	551.83	517.89
86	552.57	501.06	549.82	511.44
87	551.56	499.19	548.81	508.99
88	549.54	498.12	546.79	506.49
89	548.53	497.27	545.78	505.64
90	549	498	546.25	506
91	552.84	500.22	550.09	509.46
92	559.35	506.73	556.6	516.97
93	569.97	517.35	567.22	528.28
94	584.61	531.99	581.86	543.93
95	603.27	550.65	600.52	565.01
96	625.99	573.37	623.24	588.76
97	652.91	600.29	650.16	615.93
98	648.59	594.54	645.84	609.93
99	645.12	589.56	642.37	604.86
100	642.58	585.06	639.83	599.89
101	640.57	581.06	637.82	593.44
102	639.56	579.19	636.81	590.99
103	637.54	578.12	634.79	588.49
104	636.53	577.27	633.78	587.64
105	637	578	636	588
106	633.5	574.5	632.4	584.5
107	630	570.94	628.8	580.94
108	626.5	567.62	625.2	577.62
109	623	563.87	621.6	573.87
110	619.5	560.42	618	570.42
111	616	556.53	614.4	566.53
112	612.5	552.96	610.8	562.96
113	609	549.31	607.2	559.31
114	605.5	544.79	603.6	554.79
115	602	541.01	600	551.01
116	598.5	537.03	596.4	547.03
117	595	533.38	592.8	543.38

118	591.5	529.6	589.2	539.6
119	588	525.63	585.6	535.63
120	584.5	522.13	582	532.13
121	581	517.51	578.4	527.51
122	577.5	514.01	574.8	524.01
123	574	509.14	571.2	519.14
124	570.5	504.19	567.6	514.64
125	567	499.32	564	509.77
126	563.5	495.57	560.4	506.52
127	560	491.68	556.8	502.63
128	556.5	487.7	553.2	498.65
129	553	483.73	549.6	494.68
130	549.5	479.38	546	490.33
131	546	474.81	542.4	486.33
132	542.5	469.83	538.8	481.35
133	539	466.36	535.2	477.88
134	535.5	462.38	531.6	473.9
135	532	458.51	528	470.03
136	528.5	454.86	524.4	466.38
137	525	451.36	520.8	462.88
138	521.5	446.38	517.2	457.9
139	518	441.86	513.6	453.38
140	514.5	437.18	510	448.7
141	511	432.79	506.4	444.31
142	507.5	428.22	502.8	440.13
143	505	423.33	500.2	435.24
144	502.5	418.38	497.6	430.29
145	500	414.63	495	426.54
146	497.5	410.98	492.4	422.89
147	495	407.2	489.8	419.11
148	492.5	403.31	487.2	415.22
149	490	400.22	484.6	410.72
150	487.5	396.78	482	407.22

APPENDIX D – COPYRIGHT INFORMATION

1) Images used courtesy of ANSYS, Inc

   The following is an excerpt for the ANSYS website specifying terms and conditions on use of screenshots:

   "Academic users* of ANSYS software may make fair use of screenshots from our products in their published work. This includes but is not limited to capstone project reports, conference posters, thesis, research papers, textbooks, educational guides, video demonstrations, webpages, social media channel postings. You must include the following acknowledgement on all materials containing ANSYS product screenshots: "Images used courtesy of ANSYS, Inc."

   The link to the page is: https://www.ansys.com/academic/terms-and-conditions

2) ANSYS® Academic Research Mechanical, Release 18.2 Thermal Transient Analysis, ANSYS, Inc.

3) ANSYS® Space Claim, Release 18.2, ANSYS, Inc.

APPENDIX E – Brake Pad Models

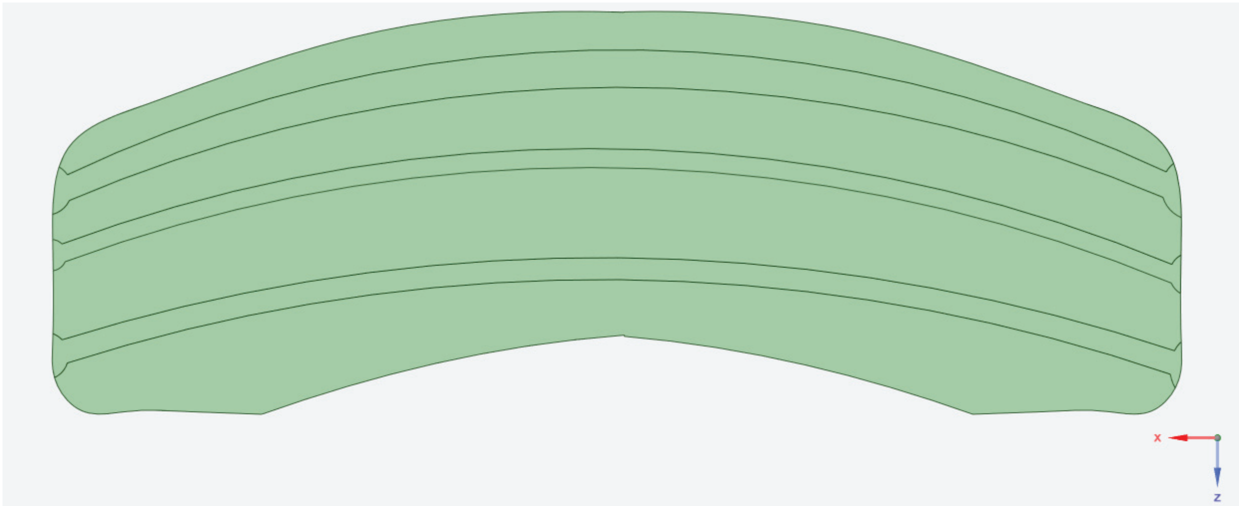

Figure 6.1.1: Modified Power Stop Brake Pad with internal Vents

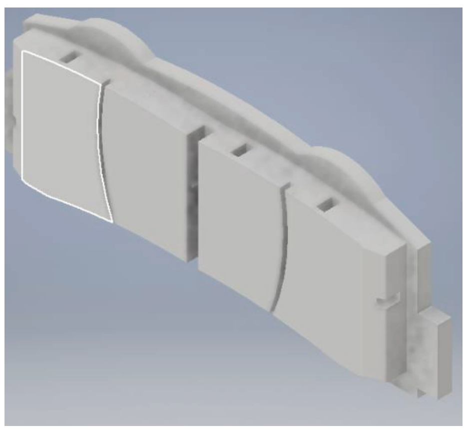

Figure 6.1.2: Top View of pad with internal Vents

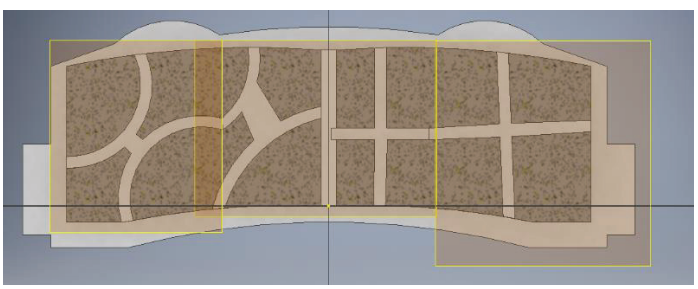

Figure 6.1.3: Internal View of Brake pad with Vents

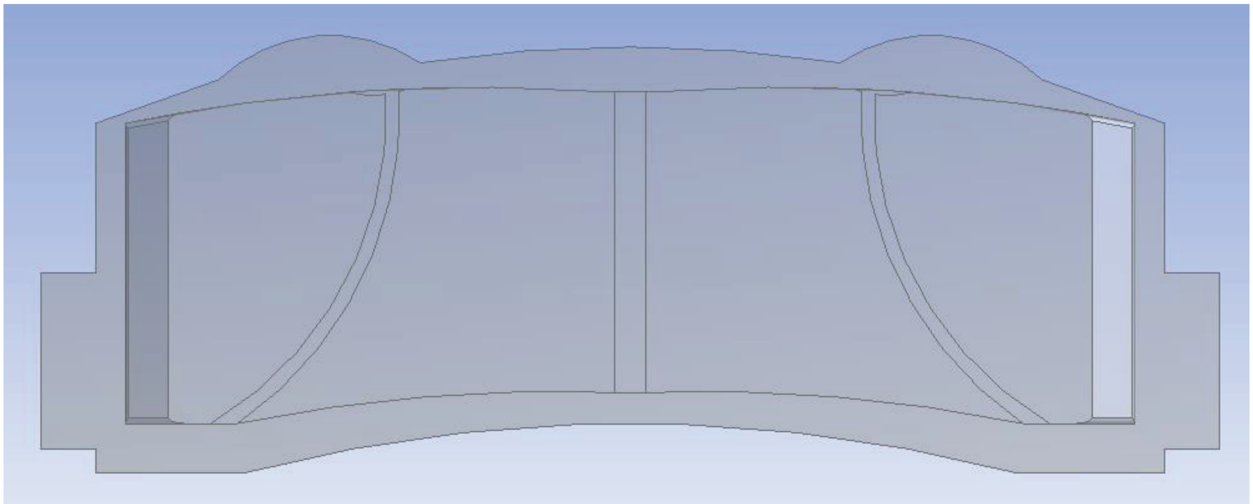

Figure 6.1.4: Brake Pad design with Non-Linear Slots

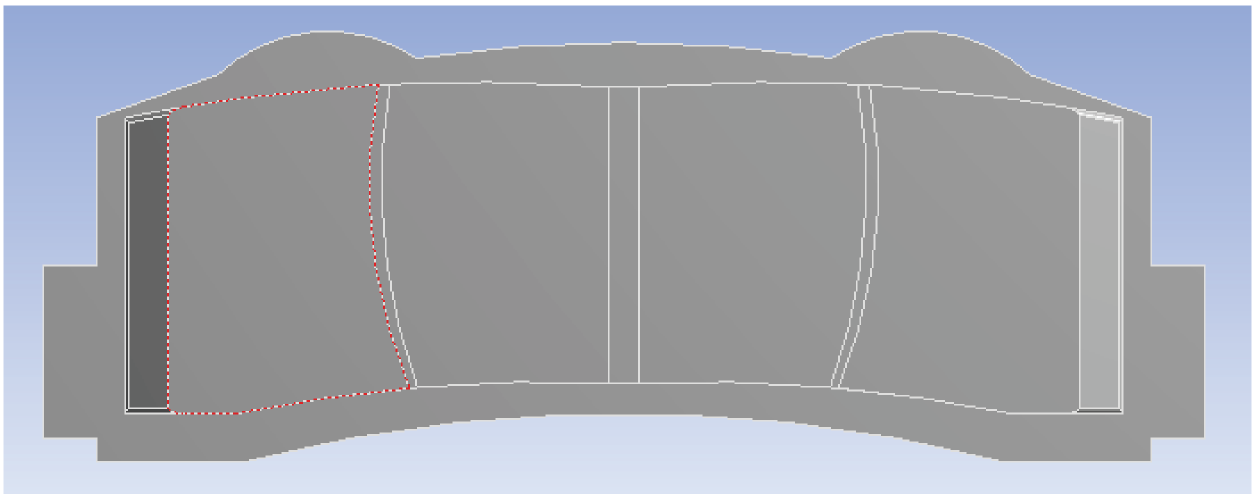

Figure 6.1.5: Brake pad design with linear slots

VITA

Graduate School

Southern Illinois University

Daryl Premkumar

darylpremkumar@siu.edu

Southern Illinois University Carbondale

Bachelor of Science, Mechanical Engineering, 2016

Thesis Title: OPTIMIZATION OF BRAKE PAD GEOMETRY TO PROMOTE GREATERCONVECTIVE COOLING TO INCREASE HEAT DISSIPATION RATE

Major Professor: Dr. Peter Filip